WAVE RADIATION FROM A TRUNCATED CYLINDER OF ARBITRARY CROSS SECTIONS

A Thesis Submitted to
the Graduate School of
İzmir Institute of Technology
in Partial Fulfillment of the Requirements for the Degree of

MASTER OF SCIENCE

in Mathematics

by
Ece Hazal KORKMAZ

December 2021
İZMİR

ACKNOWLEDGMENTS

I would like to express my sincere gratitude to my supervisor, Prof. Dr. Oğuz YILMAZ. His guidance helped me all the time during my master's studies. I want to thank him for his patience and immense knowledge.

I would also like to thank my thesis committee members Prof. Dr. Oktay PASHAEV and Doç. Dr. Ali DEMİRCİ. I am grateful for the ideas and the suggestions they shared.

My sincere thanks to Dr. Nazile Buğurcan DİŞİBÜYÜK for being so willing to help with the asymptotic approaches.

I would also like to give special thanks to Durmuş Ali UĞUR and Tuğba YAZAN and my family: my parents Figen and Atilla, my brother Aydın.

ABSTRACT

WAVE RADIATION FROM A TRUNCATED CYLINDER OF ARBITRARY CROSS SECTIONS

Wave radiation problem in heaving motion from a vertical cylinder of circular cross-section and truncated cylinder of an arbitrary cross-section in the water of finite depth is studied. First, wave radiation from the circular cylinder is summarized which was solved analytically by Yeung (1981). The water domain is divided into two regions: the interior region below the cylinder and the exterior region outside the cylinder. The interior and exterior solutions are matched by the continuity of pressure and normal velocity in both cases. The vertical cylinder of a circular cross-section is solved by using the separation of variables method in cylindrical coordinates. The coefficients of interior and exterior solutions are related by the matching conditions. The system of equations formed by these unknown coefficients has been solved. Then, the non-dimensional z component of force is calculated by integrated pressure on the floating body. The real part and imaginary parts of this force give added mass and damping coefficients in heaving motion, respectively. These numerical results are used for the verification of asymptotic solutions of the present thesis. In the second case of this thesis, we treat wave radiation problems in heaving motion from the non-circular cylinder by using an asymptotic method. The asymptotic method of this thesis was suggested by Dişibüyük et al. (2017). Dişibüyük et al. (2017) suggested the non-dimensional maximum deviation of the cylinder cross-section from a circular one plays the role of a small parameter of the problem. The third-order asymptotic solution is used. Unknown coefficients of interior and exterior potentials are solved by using Fourier coefficients at each order of approximation. The advantage of the method is that the boundary conditions can be solved for different cross-sections by using the Fourier coefficients. The results are compared with other numerical results.

ÖZET

EN KESİTİ DAİRESEL OLMAYAN KESİK BİR SİLİNDİRDEN DALGA RADYASYONU PROBLEMİ

En kesiti dairesel olan bir dik silindir ve dairesel olmayan bir dik silindirden dalma-çıkma hareketinde dalga radyasyonu problemi çalışıldı. Analitik olarak Yeung (1981) tarafından çözülen dairesel ara kesitli silindirden dalga radyasyonu problemi verildi. Su alanı iki bölgeye ayrılmıştır: silindirin altındaki iç bölge ve silindirin dışındaki dış bölge. İç ve dış bölgelerdeki çözümler basıncın ve normal hızın sürekliliğinden iki durumda da eşleştirilmiştir. Dairesel kesitli dikey silindir durumunda silindirik koordinatlarda değişkenlerin ayrılması yöntemi kullanılmıştır. İç ve dış bölgedeki çözümler eşleştirme durumundan dolayı bağlantılıdırlar. Bilinmeyen katsayıların oluşturduğu denklem sistemi çözülmüştür. Sonra, yüzen cismin üzerindeki basıncın integre edilmesiyle kuvvetin boyutsuz z bileşeni hesaplanmıştır. Kuvvetin gerçek ve sanal kısımları dalma-çıkma hareketinde sırasıyla katma kütle ve sönümleme katsayılarını verir. Bulunan sayısal sonuçlar asimptotik çözümle elde edilen sonuçların doğrulanması için kullanılmıştır. Tezin ikinci kısmında, en kesiti dairesel olmayan dik bir silindir durumu asimptotik bir yaklaşımla çözülür. Bu tezde kullanılan asimptotik yaklaşım Dişibüyük et al. (2017) tarafından önerilmiştir. Silindirin ara kesitinin, çemberden maksimum boyutsuz sapması problemin küçük bir parametresidir (Dişibüyük et al. (2017)). Problemin üçüncü mertebeden çözümü asimptotik yöntemle elde edilmektedir. İç ve dış potansiyellerin bilinmeyen katsayıları her mertebede Fourier katsayıları kullanılarak bulundu. Sınır koşullarının farklı ara kesitli silindirler için Fourier katsayıları kullanılarak çözülmesi yöntemin avantajıdır. Sonuçlar farklı en kesitli silindirler için daha önce yapılan nümerik çalışmalarla karşılaştırılmıştır.

TABLE OF CONTENTS

LIST OF FIGURES

Figure **Page**

LIST OF TABLES

Table **Page**

CHAPTER 1

INTRODUCTION

The hydrodynamic forces on fixed and floating structures or oscillating bodies are research interests for researchers and engineers. The prediction of the diffraction and the radiation forces on the structures is crucial. These structures are often used in ocean engineering, such as bridge pylons, breakwaters, offshore platforms, wave energy converters, floating offshore wind turbines and floating airports, etc.

The interaction of the incident waves with the body causes diffraction and deflection. Radiation forces come from the radiated waves generated because of the motion of the body. The floating body oscillates time-harmonically in three-dimensional space that is called six degrees of freedom. The sea waves and the movements in these waves have nonlinear characteristics. The motions of the body are assumed to have a small amplitude. The fluid flow around the floating body can be linearized by potential theory. The nonlinear and viscous effects are neglected. The mooring, which is also essential for motion control, is ignored. Linear wave theory is applied for a vertical cylinder with a constant water depth and the structure not submerged and extending to the free surface. Truncated cylinders are mostly used in ocean engineering as wave energy converters (Zheng and Zhang (2018)), spar platforms (Sudhakar and Nallayarasu (2011)), elliptic and quasi-elliptic sectional bridge's foundations (Liu et al. (2016), Eidem (2017), Liu et al. (2018)). Also, Wan et al. (2017) studied numerical models on bridges floating on pontoons that are the form of multiple elliptical cylinders.

An analytical solution to the problem of wave radiation from the circular cross-section cylinder was proposed by Yeung (1981). The method was used before by Garrett (1971) that was discussed the scattering of surface gravity waves by a circular dock. The radius of the circular section was r=a, and the interior region was defined as r<a and the exterior region as r>a, respectively. The inner and outer region problems were written as potential functions in Dirichlet and Neumann types, respectively. Incident waves expanded in Bessel functions. After that unknown coefficients were solved by matching their normal velocities at r=a. The fact that the geometry was axisymmetric in circular

shape allowed the problem to be solved more easily. Black et al. (1971) used Haskind's theorem (Haskind (1957)) to the wave forces on a stationary body problem. In this case, the far-field properties were sufficient. The study didn't include direct calculations for radiation forces. Yeung (1981) divided region into two parts: interior and exterior regions to determine velocity potential. Eigenfunctions of these problems were matched and the separation of variables method was used to find the unknown coefficients. Added mass and damping for heave motion were computed and presented for the different radius to depth and the bottom clearance to depth ratios. The velocity potentials were represented in terms of Bessel and modified Bessel functions. These numerical results are used for the asymptotic solutions of the present thesis. In another study, Drobyshevski (2004) obtained hydrodynamic coefficients for a circular truncated cylinder for extremely shallow water by using asymptotic methods. The distance between the bottom surface of the cylinder and the seabed was very small and this small distance is used for asymptotic expansions. Then, asymptotic expansions of potentials in the common region were matched. The author stated that as the distance under the cylinder decreases, the heave added mass rises rapidly and is affected depending on the water depth. However, at the same depth, radiation damping was weakly affected. Results were in agreement with Yeung (1981). Later, Bhatta (2007) studied the effect of water depth and draft on hydrodynamics. The results showed that the heave added mass was greater for the higher draft for cylinders with the same water depth.

Studies on structures with non-circular cross-sections were examined by Chen and Mei (1971), Williams and Darwiche (1990), Lee (1995), Yu et al. (2019). The scattering and radiation from elliptical cylinder were studied by Chen and Mei (1971) that used the separation of variables method in the elliptical coordinate system and representing the velocity potential in terms of infinite series of Mathieu and modified Mathieu functions. Williams and Darwiche (1990) studied wave radiation from an elliptical cylinder in two cases: cylinder was submerged or floating on the free surface. In their study, a theoretical solution was given for the radiation of small-amplitude water waves. The numerical results are presented for the added mass and damping coefficients for truncated elliptical cylinders with different eccentricities and drafts. Again, velocity potential in elliptical coordinates was written as Mathieu functions. Lee (1995) analytically solved the heave radiation problem for the rectangular structure. But this problem was in two-dimension.

Lee (1995) also solved the problem with the boundary element method to compare, and the results were very close. They pointed about that the added mass coefficient increase if the width of the structure and the water depth increase, the radiation damping increase if the width of the structure increase. Yu et al. (2019) extended their studies to cylinders with a different cross-section and, they suggested a semi-analytical solution for radiation problem. The method for finding unknown hydrodynamic coefficients by matching velocities in the common region was the same as in other studies. However, the radius function was defined in cylindrical coordinates and the boundary conditions are solved by writing the radius function into the Fourier series. Added mass and damping were calculated for cylinders with circular, cosine, elliptical, and quasi-elliptical cross-sections with the same depth and same cross-sectional area (Yu et al. (2019)). The numerical results for cosine type radial perturbation were calculated by using the Boundary Element Method and the ANSYS AQWA software showed excellent agreement with the semi-analytical method. Added mass and damping for the quasi-elliptic type were calculated in different drafts. The results were used to compare with the asymptotic approaches obtained in this thesis.

The asymptotic solution of wave diffraction from a bottom-mounted vertical cylinder with different cross-sections was presented by Dişibüyük et al. (2017) using the fifth-order approximation which has good agreement with cosine type cross-section by Liu et al. (2016). The asymptotic method in their work was proposed by Mei et al. (2005). The method is useful for structures with arbitrary cross-sections. Mansour et al. (2002) expressed the diffraction problem for a vertical cylinder with cosine type cross-section as a series dependent on the perturbation parameter of the velocity potential. The series expansion of the velocity potential was written in the boundary conditions and the zeroth and first-order equation systems were obtained. They continued with numerical calculations such as the integral equation method and the Green functions. The zeroth-order system was the same as the circular cylinder case. The integral equation method and the asymptotic method were closed when the perturbation amplitude was small. Liu et al. (2016) solved the diffraction problem by expanding the radius function and boundary conditions on the surface of the cylinder to the Fourier series of Bessel and Hankel functions. Dişibüyük et al. (2017) suggested velocity potential and shape function in terms of Fourier series and applied fifth-order approximation to the diffraction problem for cylinders with arbitrary cross-section such as elliptic, square, quasi-elliptic, cosine type. Asymptotic

results are close to other numerical and experimental results. The asymptotic method of this thesis was suggested by Dişibüyük et al. (2017).

Computational methods were reviewed by Mei (1978) for diffraction and radiation problems. The first method was the method of the integral equation using Green's functions. The second method was the Hybrid element method which was based on the finite element method. The author noted that the calculations are more practical when compared to the integral equation method. Numerical simulations were also used in the wave radiation problem. For example, Yu et al. (2019) compared the results obtained with the semi-analytical method using the boundary element method. In another article, Islam et al. (2019) used OpenFOAM analysis for box-type oscillating structures. They achieved very close results with analytical solutions. They noted that CFD for box-type structures is suitable for interaction problems. Especially, it can be used for wave energy converters.

Wave radiation problem can be also extended to different conditions such as circular cylinder in a channel (Linton et al. (1992)), a rectangular structure with a sidewall (Zheng et al. (2004)), rectangular structure over a sill (Shen et al. (2005)), floating rectangular structure in oblique seas (Zheng et al. (2006)), cylinder in front of a vertical wall (Zheng and Zhang (2016)), submerged cylinder in finite water (Jiang et al. (2014)), submerged elliptical disk (Zhang et al. (1995)), etc.

In this thesis, wave radiation problem in heaving motion from a vertical cylinder of circular cross-section and truncated cylinder of an arbitrary cross-section in the water of finite depth is studied. First, wave radiation from the circular cylinder is summarized which is studied before (Yeung (1981)). The water domain is divided into two regions: the interior region below the cylinder and the exterior region outside the cylinder. The interior and exterior solutions are matched by the continuity of pressure and normal velocity in both cases. The vertical cylinder of a circular cross-section is solved by using the separation of variables method in cylindrical coordinates. The coefficients of interior and exterior solutions are related by the matching conditions. The system of equations formed by these unknown coefficients has been solved. Then, the non-dimensional z component of force is calculated by integrated pressure on the floating body. The interior solution is used to calculate the force. The real part and imaginary parts of this force give added mass and damping coefficients in heaving motion, respectively. The added mass and the damping coefficients are proportional to acceleration and the body velocity, respectively.

These numerical results are used for the verification of asymptotic solutions of the present thesis. In the second case of this thesis, we treat wave radiation problems in heaving motion from the non-circular cylinder. We studied by using an asymptotic method which was suggested by Dişibüyük et al. (2017). The non-dimensional maximum deviation of the cylinder cross-section from a circular one plays the role of a small parameter of the problem as in the paper by Dişibüyük et al. (2017). A third-order asymptotic solution of the problem is obtained as in the paper by Dişibüyük et al. (2017). Unknown coefficients of interior and exterior potentials are solved by using Fourier series of the shape function at each order of approximation. The advantage of the method is that the boundary conditions can be solved for different cross-sections by using the Fourier coefficients. The asymptotic approach is applied for cylinders with different cross-sections such as elliptic, quasi-elliptic, square, and cosine cross-section. The computational results are compared with other studies.

The structure of the thesis is as follows:

In Chapter 2, some fundamentals of fluid dynamics such as incompressibility condition, Euler's equation, potential flow theory, and Bernoulli's equation for unsteady irrotational flow are given. The boundary conditions are presented. The body response in regular waves are given.

In Chapter 3, the wave radiation problem in heaving motion by a vertical cylinder of the circular cross-section is solved by separation of variables method in cylindrical coordinates. The coefficients of interior and exterior solutions are related to each other by the matching conditions which are based on the study of Yeung (1981). The matrix system formed by these unknown coefficients has been solved. Then, the non-dimensional z component of force is calculated. Real part and imaginary parts of F_z give added mass and damping coefficients in heaving motion, respectively. Added mass and damping for $0 < k_0 a < 4$ presented for different values of radius a and the distance d between sea bottom and cylinder's bottom surface.

In Chapter 4, the wave radiation problem in heaving motion by a vertical cylinder of an arbitrary cross-section is solved by an asymptotic approach. The radius of the cross-section of the vertical cylinder is described by the equation $r = R[1 + \varepsilon f(\theta)]$ where R is the mean radius of the cylinder and ε be the small non-dimensional parameter of the problem (Dişibüyük et al. (2017)). Wave radiation in heaving motion from a vertical cylinder is

studied by the third-order asymptotic method. The interior and exterior potentials, shape functions are written in terms of the Fourier Series. Non-dimensional added mass and damping coefficients are compared for cylinders with circular, cosine type, square, elliptic, and quasi-elliptic cross-section with the other numerical results. The presented results compared with the numerical results of Williams and Darwiche (1990) and Yu et al. (2019).

In Chapter 5, the conclusion is shown.

CHAPTER 2

FUNDAMENTALS OF HYDRODYNAMICS

2.1. Equations of Motion

In this section, we introduce some elementary equations of fluid dynamics. The ideal fluid defined as (Acheson (2005))

- The fluid is incompressible,
- The density of the fluid is a constant which is not change with time.
- The force on the surface element $\mathbf{n}\partial S$ in the fluid is

$$p\mathbf{n}\partial S \tag{2.1}$$

where the pressure $p(x, y, z, t)$ is constant.

Consider a surface S drawn in the fluid which is fixed and closed with unit outward normal $\mathbf{n}$. Fluid will be entering the enclosed region V on S, and leaving it. The velocity component along the $\mathbf{n}$ is $\mathbf{u} \cdot \mathbf{n}$ and the volume of fluid leaving through ∂S in unit time is $\mathbf{u} \cdot \mathbf{n}\partial S$ (Acheson (2005)). The net volume rate of leaving fluid is

$$\int_S \mathbf{u} \cdot \mathbf{n} dS \tag{2.2}$$

The equation (2.2) should be zero for an ideal fluid and by the divergence theorem, we have

$$\int_S \nabla \cdot \mathbf{u} dS = 0 \tag{2.3}$$

The equation is satisfied on the region and incompressibility gives

$$\nabla \cdot \mathbf{u} = 0 \tag{2.4}$$

everywhere in the fluid.

2.2. Euler's Equation

The equations (2.5) and (2.6) are known as Euler's equations for an ideal fluid:

$$\frac{D\mathbf{u}}{Dt} = -\frac{1}{\rho}\nabla p + \mathbf{g} \tag{2.5}$$

$$\nabla \cdot \mathbf{u} = 0 \tag{2.6}$$

where $\mathbf{g} = (0, 0, -g)$ is the graviational term and it can be written as

$$\mathbf{g} = -\nabla\chi \quad \text{since} \quad \chi = gz \tag{2.7}$$

We can rearrange equation (2.5) and we get

$$\frac{\partial \mathbf{u}}{\partial t} + (\mathbf{u} \cdot \nabla)\mathbf{u} = -\nabla\left(\frac{p}{\rho} + \chi\right) \tag{2.8}$$

since the density ρ is constant. The vector identity can be substituted into equation (2.8),

$$(\mathbf{u} \cdot \nabla)\mathbf{u} = (\nabla \wedge \mathbf{u}) \wedge \mathbf{u} + \nabla\left(\frac{1}{2}|\mathbf{u}|^2\right) \tag{2.9}$$

and we get the momentum equation into the form

$$\frac{\partial \mathbf{u}}{\partial t} + (\nabla \wedge \mathbf{u}) \wedge \mathbf{u} = -\nabla\left(\frac{p}{\rho} + \frac{1}{2}|\mathbf{u}|^2 + \chi\right) \tag{2.10}$$

2.3. Potential Flow

The vorticity equation $\omega = \nabla \wedge \mathbf{u}$ is zero for an irrotational flow, then we can say that the velocity potential ϕ exists and defined at point P by

$$\phi = \int_O^P \mathbf{u} \cdot \mathbf{x} \tag{2.11}$$

where O is arbitrary point. The potential ϕ is independent in the simpliy connected fluid region and the path between the points O and P. The equation (2.11) gives

$$\mathbf{u} = \nabla\phi \tag{2.12}$$

If incompressible, inviscid and irrotational flow is assumed, then we can define velocity potential ϕ. The incompressibility condition in (2.6) provides the potential ϕ satisfy Laplace equation.

$$\nabla^2\phi = 0 \tag{2.13}$$

2.4. Bernoulli's Equation

Irrotational flow is assumed and $\mathbf{u}$ can be written as gradient of velocity potential, i.e, $\mathbf{u} = \nabla\phi$. So, Euler's equation (2.10) becomes

$$\frac{\partial(\nabla\phi)}{\partial t} = -\nabla\left(\frac{p}{\rho} + \frac{1}{2}|\mathbf{u}|^2 + \chi\right) \quad \text{since} \quad \nabla \wedge \nabla\phi = 0 \tag{2.14}$$

After integration of (2.14), we get Bernoulli's equation for unsteady irrotational flow:

$$\frac{\partial\phi}{\partial t} + \frac{p}{\rho} + \frac{1}{2}|\mathbf{u}|^2 + \chi = G(t) \tag{2.15}$$

where G is a time-dependent arbitrary function.

2.5. Boundary Conditions

The fluid motion appears from a deformation of the water surface and free surface equation can be denoted by

$$z = \eta(x, y, t) \tag{2.16}$$

2.5.1. Kinematic Condition at the Free Surface

Fluid particles on the surface have to stay on the surface. Let assume that $F(x, y, z, t)$ stays constant for any particular particle on the free surface and $F(x, y, z, t) = z - \eta(x, y, t)$. In other words, $DF/Dt = 0$ on the free surface, i.e.

$$\frac{\partial F}{\partial t} + (\mathbf{u} \cdot \nabla)F = 0 \quad \text{on} \quad z = \eta(x, y, t) \tag{2.17}$$

2.5.2. The Pressure Condition at the Free Surface

Inviscid flow is assumed and pressure p at free surface is equal to atmospheric pressure P_0 at $z = \eta(x, y, t)$. If we assume that the P_0 and density are constant and choose $G(t)$ accordingly, we can rewrite equation (2.15) to simplify it, i.e.

$$\frac{\partial \phi}{\partial t} + \frac{1}{2}|\mathbf{u}|^2 + g\eta = 0 \quad \text{on} \quad z = \eta(x, y, t) \tag{2.18}$$

2.5.3. Linearization of the Surface Waves

Suppose that both free surface displacement η and fluid velocities $\mathbf{u}$ are small. We can linearize the problem ignoring quadratic and higher terms. Moreover, expanding equation (2.17) in a Taylor series at $z = \eta$ and ignoring quadratic and higher terms, we have

$$\frac{\partial \phi}{\partial z} = \frac{\partial \eta}{\partial t} \quad \text{on} \quad z = h \tag{2.19}$$

Similarly, the pressure condition (2.18) gives

$$\frac{\partial \phi}{\partial t} + g\eta = 0 \quad \text{on} \quad z = h \tag{2.20}$$

2.5.4. Body Boundary Conditions

The boundary can be fixed and rigid. Let rigid body moving with velocity **u** through the fluid, the velocity of this surface is nonzero. The normal compenent of fluid velocity must be equal to the normal velocity of the boundary surface itself. The fluid cannot flow through the boundary surface (Newman (2018)). Boundary condition becomes

$$\frac{\partial \phi}{\partial \mathbf{n}} = \mathbf{u} \cdot \mathbf{n} \tag{2.21}$$

where **n** is the unit normal vector directed out of the fluid.

2.6. Body Response in Waves: Added Mass and Damping

The interaction of the incident waves with the body causes diffraction and deflection. Radiation forces come from the radiated waves generated because of the motion of the body. The floating body oscillates time-harmonically in three-dimensional space that is called six degrees of freedom. We define three translational motions parallel to $(x, y, z) = (x_1, x_2, x_3)$ as surge, sway, and heave, and three rotational motions about the same axes as roll, pitch, and yaw, respectively (Newman (2018)). The velocity will be sinusodial in time, we get

$$U_j(t) = \mathrm{Re}[i\sigma\xi_j e^{i\sigma t}], \;\; j = 1, 2, \ldots, 6. \tag{2.22}$$

where ξ_j is the amplitude. The wave amplitude is small to justify linearization. The velocity potential can be written in the form

$$\Phi(x, y, z, t) = \mathrm{Re}\left[\sum_{j=1}^{6} (\xi_j \phi_j(x, y, z) + A\phi_A) e^{i\sigma t}\right] \tag{2.23}$$

where ϕ_j is the potential of a rigid body motion with unit amplitude and it is the solutions of the radiation problem for $j = 1, 2, \ldots, 6$.

$$\frac{\partial \phi_j}{\partial n} = i\sigma n_j, \;\; j = 1, 2, 3. \tag{2.24}$$

$$\frac{\partial \phi_j}{\partial n} = i\sigma(\mathbf{r} \times \mathbf{n})_{j-3}, \;\; j = 4, 5, 6. \tag{2.25}$$

on the body surface S. The unit normal vector is **n** and the position vector is **r**.

$$\frac{\partial \phi_A}{\partial n} = 0, \;\; \text{on} \quad \text{S} \tag{2.26}$$

$$\phi_A = \phi_0 + \phi_7 \tag{2.27}$$

where ϕ_0 is the incident wave potential and ϕ_7 is the scattering potential. This problem defined as diffraction problem. Also, each potential satisfy Laplace's equation.

$$\nabla^2 \phi_j = 0, \;\; j = 0, 1, 2, \ldots, 7. \tag{2.28}$$

The linearized boundary condition gives

$$-\frac{\sigma^2}{g}\phi_j + \frac{\partial \phi_j}{\partial z} = 0, \;\; \text{on } z = h, \;\; j = 0, 1, 2, \ldots, 7. \tag{2.29}$$

The radiation condition gives

$$\phi_j \propto (x^2 + y^2)^{1/2} e^{-ikR}, \;\; \text{as } (x^2 + y^2)^{1/2} \to \infty, \;\; j = 1, 2, \ldots, 7. \tag{2.30}$$

The equation (2.23) is substituted into unsteady Bernoulli's equation. The quadratic and higher terms are ignored. The total pressure is given by

$$\begin{aligned} p &= -\rho\left(\frac{\partial\phi}{\partial t} + gz\right) \\ &= -\rho Re\left[\sum_{j=1}^{6}(\xi_j\phi_j + A(\phi_0 + \phi_7))i\sigma e^{i\sigma t}\right] - \rho gz \end{aligned} \tag{2.31}$$

The force **F** and moment **M** can be determined by integrating the fluid pressure over the wetted surface S (Newman (2018)).

$$\begin{aligned} \begin{pmatrix} \mathbf{F} \\ \mathbf{M} \end{pmatrix} &= -\rho g \iint_S \begin{pmatrix} \mathbf{n} \\ \mathbf{r}\times\mathbf{n} \end{pmatrix} z dS - \rho \mathrm{Re}\sum_{j=1}^{6} i\sigma\xi_j\phi_j e^{i\sigma t} \iint_S \begin{pmatrix} \mathbf{n} \\ \mathbf{r}\times\mathbf{n} \end{pmatrix}\phi_j dS \\ &\quad - \rho \mathrm{Re} i\sigma A e^{i\sigma t} \iint_S \begin{pmatrix} \mathbf{n} \\ \mathbf{r}\times\mathbf{n} \end{pmatrix}(\phi_0 + \phi_7) dS \end{aligned} \tag{2.32}$$

The hydrostatic force in the form

$$\mathbf{F} = -\rho g \iint_S \mathbf{n} z dS \tag{2.33}$$

and moment in the form

$$\mathbf{M} = -\rho g \iint_S (\mathbf{r}\times\mathbf{n}) z dS \tag{2.34}$$

The components of force and moment can be written as

$$F_i = \mathrm{Re}\sum_{j=1}^{6} i\sigma\xi_j e^{i\sigma t} f_{ij},\ i = 1, 2, \ldots, 6. \tag{2.35}$$

where

$$f_{ij} = -\rho \iint_S \frac{\partial\phi_i}{\partial n}\phi_j dS \tag{2.36}$$

The coefficient f_{ij} is the complex force in the direction i, due to a sinusodial motion of unit amplitude in the direction j.

$$f_{ij} = \sigma^2 a_{ij} - i\sigma b_{ij} \tag{2.37}$$

The added mass coefficient is a_{ij} which gives the force component proportional to the acceleration. The damping coefficient is b_{ij} which gives the force component proportional to the body velocity. These boundary conditions, real and imaginary parts of the force are required for the radiation problem.

CHAPTER 3

WAVE RADIATION IN HEAVING MOTION FROM A VERTICAL CYLINDER OF CIRCULAR CROSS SECTION

Wave radiation from a floating vertical circular cylinder in finite-depth water is studied analytically by Yeung (1981). The region is divided into two regions by Yeung (1981): interior and exterior regions to determine velocity potential. Solutions for interior and exterior problems are obtained by the separation of variables method. Eigenfunctions of these problems are matched to find the unknown coefficients. Added mass and damping for heave motion are computed and presented for the different radius to depth and the bottom clearance to depth ratios. The velocity potentials were represented in terms of Bessel and modified Bessel functions. These numerical results are used for the asymptotic solutions of the present thesis.

3.1. Mathematical Formulation

In this problem, we formulated boundary value problem for heaving of a vertical cylinder with circular cross-section in finite depth water $\bar{h}$. Seabed is horizontal and fixed. Let the Oxy plane be the sea bottom, $(\bar{r}, \theta)$ be polar coordinates, and the z-axis point upwards. Gravitational acceleration g is in z direction. The cylinder extends from $\bar{d}$ to the free surface. The floating body oscillates time-harmonically along the z-axis. If incompressible, irrotational and inviscid fluid flow is assumed, the velocity potential $\Phi(\bar{r}, \theta, \bar{z}, t)$ as given:

$$\Phi = U_3 \bar{\phi}_3 \tag{3.1}$$

$$U_3(t) = \frac{dX_3}{dt} = Re[-i\sigma\bar{\xi}_3 e^{-i\sigma t}] \,, \quad where \quad X_3 = \bar{\xi}_3 \cos(\sigma t) \tag{3.2}$$

$$\Phi = Re[-i\sigma\bar{\xi}_3 e^{-i\sigma t}\bar{\phi}_3(\bar{r}, \theta, \bar{z})] \tag{3.3}$$

where σ is the angular frequency, $\bar{\xi}_3$ the heave amplitude, X_3 the displacement function, U_3 the heave velocity, and $i = \sqrt{-1}$. Note that the dimensions of Φ, U_3, σ, $\bar{\xi}_3$, and $\bar{\phi}_3$ are L^2/T, L/T, $1/T$, L and L, respectively. Velocity potential satisfies Laplace equation and

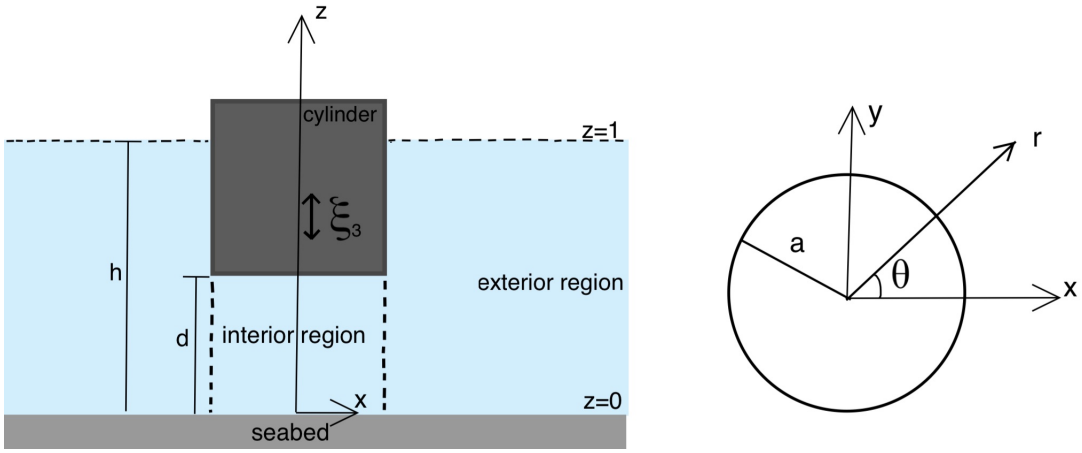

Figure 3.1. Coordinate system and notations

boundary conditions on free surface, sea bottom and body:

$$\nabla^2\Phi = 0$$

$$\frac{\partial\Phi}{\partial z} = \frac{\partial\eta}{\partial t} \quad \text{on } \bar{z} = \bar{h} \quad \text{(Kinematic Condition)}$$

$$\frac{\partial\Phi}{\partial t} + g\eta = 0 \quad \text{on } \bar{z} = \bar{h} \quad \text{(Dynamic Condition at } p = P_0\text{)}$$

$$\frac{\partial\Phi}{\partial z} + \frac{1}{g}\frac{\partial^2\Phi}{\partial t^2} = 0 \quad \text{on } \bar{z} = \bar{h} \quad \text{(Combined D.C. and K.C.)}$$

$$\frac{\partial\Phi}{\partial z} = 0 \quad \text{at } \bar{z} = 0$$

$$\frac{\partial\Phi}{\partial n} = \nabla\Phi \cdot \mathbf{n} = U_3(t) \cdot n_z \quad \text{on } \bar{z} = \bar{d},\ 0 \le \bar{r} \le \bar{a}$$

$$\frac{\partial\Phi}{\partial n} = \nabla\Phi \cdot \mathbf{n} = 0 \quad \text{at } \bar{r} = \bar{a}, \quad \bar{d} \le \bar{z} \le \bar{h}$$

$$\Phi \to 0 \quad \text{as} \quad \bar{r} \to \infty \quad \text{(Radiation Condition)}$$

$\eta(\bar{r}, \theta, t)$ defines free surface function, P_0 athmospheric pressure. The potential Φ is finite at $\bar{r} = 0$.

In this case, fluid motion has axisymmetric behaviour. In the paper Yeung (1981), all space variables are non-dimensionalized by water depth $\bar{h}$. For example, a represents the radius to water-depth ratio ($\bar{a}/\bar{h}$); d the bottom clearance to water-depth ratio ($\bar{d}/\bar{h}$). The non-dimensional form of potential $\bar{\phi}_3(=\bar{h}\phi)$ provides

$$\Phi(r,\theta,z,t) = \bar{h}Re[-i\sigma\bar{\xi}_3 e^{-i\sigma t}\phi(r,z)] \tag{3.4}$$

$$\nabla^2\phi = 0 \tag{3.5}$$

$$\frac{\partial\phi}{\partial z} - \nu\phi = 0 \quad \text{on } z = 1, \quad \nu = \frac{\sigma^2}{g}\bar{h} \tag{3.6}$$

$$\frac{\partial\phi}{\partial z} = 0 \quad \text{at } z = 0 \tag{3.7}$$

$$\frac{\partial\phi}{\partial z} = 1 \quad \text{on } z = d, \quad 0 \le r \le a \tag{3.8}$$

$$\frac{\partial\phi}{\partial r} = 0 \quad \text{at } r = a, \quad d \le z \le 1 \tag{3.9}$$

$$\phi \to 0 \quad \text{as} \quad r \to \infty \tag{3.10}$$

The potential ϕ is finite at $r = 0$.

We will separate the region into two parts: interior and exterior regions. The solution $\phi^{(i)}(r,z)$ in the interior region ($r \le a$) is below the cylinder ($0 \le z \le d$) and the solution $\phi^{(e)}(r,z)$ in the exterior region ($r \ge a$) is outside of the cylinder ($0 \le z \le 1$) as in the paper by Yeung (1981).

3.1.1. Inner Solution

The interior solution satisfies the equations (3.5), (3.7), and (3.8). It can be expressed as a sum of homogeneous and particular solutions to solve the inhomogeneous boundary value problem which comes from the cylinder's bottom surface.

$$\phi^{(i)} = \phi_h^{(i)} + \phi_p^{(i)} \tag{3.11}$$

where $\phi_h^{(i)}$ and $\phi_p^{(i)}$ satisfy the following boundary conditions:

$$\left.\frac{\partial\phi_h^{(i)}}{\partial z}\right|_{z=0} = 0, \qquad \left.\frac{\partial\phi_h^{(i)}}{\partial z}\right|_{z=d} = 0 \tag{3.12}$$

$$\left.\frac{\partial \phi_p^{(i)}}{\partial z}\right|_{z=0} = 0, \qquad \left.\frac{\partial \phi_p^{(i)}}{\partial z}\right|_{z=d} = 1 \tag{3.13}$$

Separation of variables method is applied to get the solution of the differential equation. We have homogeneous and inhomogeneous parts. The potential $\phi_h^{(i)}$ satisfies the Helmholtz equation,

$$\phi_{h,rr}^{(i)} + \frac{1}{r}\phi_{h,r}^{(i)} - \lambda_j^2 \phi_h^{(i)} = 0, \quad \lambda_j = \frac{j\pi}{d} \tag{3.14}$$

Then we have:

$$\phi_p^{(i)} = \frac{1}{2d}\left(z^2 - \frac{r^2}{2}\right) \tag{3.15}$$

$$\phi_h^{(i)} = \frac{\alpha_0}{2} + \sum_{j=1}^{\infty} \alpha_j \frac{I_0(\lambda_j r)}{I_0(\lambda_j a)} \cos(\lambda_j z), \quad \lambda_j = \frac{j\pi}{d} \tag{3.16}$$

where α_j are Fourier coefficients and I_0 is the modified Bessel function of the first kind order zero since the interior potential ϕ is finite at $r = 0$. Hence interior solution is

$$\phi^{(i)}(r,z) = \frac{1}{2d}\left(z^2 - \frac{r^2}{2}\right) + \frac{\alpha_0}{2} + \sum_{j=1}^{\infty} \alpha_j \frac{I_0(\lambda_j r)}{I_0(\lambda_j a)} \cos(\lambda_j z), \quad \lambda_j = \frac{j\pi}{d} \tag{3.17}$$

where $r \leq a$ and $0 \leq z \leq d$.

The coefficients α_j are not known at the moment. We need the exterior solution and matching conditions which are given in Sections 3.1.2 and 3.1.3.

3.1.2. Exterior Solution

The exterior solution satisfies equations (3.5), (3.6), (3.7), (3.9) and (3.10). We used separation of variables method to obtain the exterior solution $\phi^{(e)}$. The exterior solution can be written as

$$\phi^{(e)}(r,z) = \sum_{\ell=0}^{\infty} A_\ell R_\ell(k_\ell r) Z_\ell(k_\ell z) \tag{3.18}$$

where $r \geq a$ and $0 \leq z \leq 1$. The coefficients A_ℓ are unknown coefficients and k_ℓ are solutions of the relations $k_0 tanh(k_0) = v$ and $k_\ell tan(k_\ell) = -v$, $\ell \geq 1$. The potential $\phi^{(e)}(r, z)$ satisfies Helmholtz equation,

$$\phi^{(e)}_{rr} + \frac{1}{r}\phi^{(e)}_r + k^2\phi^{(e)} = 0, \tag{3.19}$$

$$\phi^{(e)}_{rr} + \frac{1}{r}\phi^{(e)}_r - k^2\phi^{(e)} = 0, \tag{3.20}$$

The functions R_ℓ given by

$$R_\ell(k_\ell r) = \begin{cases} H^{(1)}_0(k_0 r), & \text{for } \ell = 0 \\ K_0(k_\ell r), & \text{for } \ell \geq 1 \end{cases} \tag{3.21}$$

where $H^{(1)}_0$ is the Hankel function of order zero, and K_0 is the Macdonald function of order zero since the radiation condition.

$$Z_\ell(k_\ell z) = \begin{cases} \cosh(k_0 z)/N_0^{1/2}, & N_0 = \frac{1}{2}\left(1 + \frac{\sinh(2k_0)}{2k_0}\right) \\ \cos(k_\ell z)/N_\ell^{1/2}, & N_\ell = \frac{1}{2}\left(1 + \frac{\sin(2k_\ell)}{2k_\ell}\right) \end{cases} \tag{3.22}$$

The function Z_ℓ is normalized orthogonal set in [0,1] (see Appendix A).

3.1.3. Matching Conditions

The potentials $\phi^{(i)}(r, z)$ and $\phi^{(e)}(r, z)$ are matched at $r = a$ by the continuity of pressure and their normal velocities are same at $r = a$ and $0 \leq z \leq d$ by the continuity of normal velocity between interior and exterior regions.

$$\phi^{(e)}(a, z) = \phi^{(i)}(a, z) \tag{3.23}$$

$$\left.\frac{\partial\phi^{(e)}}{\partial r}\right|_{r=a} = \left.\frac{\partial\phi^{(i)}}{\partial r}\right|_{r=a} \tag{3.24}$$

Using the body boundary condition (3.9) and matching the velocities of $\phi^{(e)}$ and $\phi^{(i)}$ at $r = a$ (3.24) gives:

$$\sum_{\ell=0}^{\infty} k_\ell A_\ell R_\ell^{'}(k_\ell a) Z_\ell(k_\ell z) = \begin{cases} 0, & d \le z \le 1 \\ \phi_r^{(i)}(a,z), & 0 \le z \le d \end{cases} \tag{3.25}$$

where the prime and the subscript r denote the differentiation with respect to r. We can multiply given piecewise function with $Z_\ell(k_\ell z)$, $\ell = 0, 1, 2, ...$ then integrate from 0 to 1:

$$\int_0^1 k_\ell A_\ell R_\ell^{'}(k_\ell a)[Z_\ell(k_\ell z)]^2 dz = \int_0^d \frac{\partial}{\partial r}\phi^{(i)}(a,z) Z_\ell(k_\ell z) dz \tag{3.26}$$

Using the orthonormal properties of the Z_ℓ (see Appendix A), we obtain:

$$k_\ell A_\ell R_\ell^{'}(k_\ell a) = \int_0^d \frac{\partial}{\partial r}\phi^{(i)}(a,z) Z_\ell(k_\ell z) dz \tag{3.27}$$

After some calculations, we get:

$$A_\ell = \left(A_\ell^* + \sum_{j=0}^{\infty} \alpha_j S_j E_{j\ell} \right) / k_\ell R_\ell^{'} \qquad \ell = 0, 1, 2, ... \tag{3.28}$$

The quantity S_j is given by:

$$S_j = \frac{j\pi}{2} \frac{I_0^{'}(\lambda_j a)}{I_0(\lambda_j a)}, \quad \lambda_j = \frac{j\pi}{d} \tag{3.29}$$

The unknown coefficient A_ℓ^* comes from integration of inhomogeneous boundary condition of interior solution. The integrals A_ℓ^* and $E_{j\ell}$, $j = 0, 1, 2...$, $\ell = 0, 1, 2...$ are defined by:

$$A_\ell^* = \int_0^d \frac{\partial}{\partial r}\phi_p^{(i)}(a,z) Z_\ell(k_\ell z) dz = \begin{cases} \frac{-a\sinh(k_0 d)}{2dk_0 N_0^{1/2}}, & \ell = 0 \\ \frac{-a\sin(k_\ell d)}{2dk_\ell N_\ell^{1/2}}, & \ell \ge 1 \end{cases} \tag{3.30}$$

$$E_{j\ell} = \frac{2}{d}\int_0^d \cos(\lambda_j z) Z_\ell(k_\ell z) dz = \begin{cases} \frac{2(-1)^j \sinh(k_0 d)}{k_0 d\left[1+\left(\frac{j\pi}{dk_0}\right)^2\right] N_0^{1/2}}, & \ell = 0 \\ \frac{2\sin(k_\ell d - j\pi)}{(k_\ell d - j\pi) N_\ell^{1/2}} \frac{k_\ell d}{(k_\ell d + j\pi)}, & \ell \ge 1 \end{cases} \tag{3.31}$$

Using equality of potentials $\phi^{(e)}$ and $\phi^{(i)}$ at r=a (3.23) we have:

$$\frac{\alpha_0}{2} + \sum_{j=1}^{\infty} \alpha_j \cos(\lambda_j z) = \phi^{(e)}(a,z) - \frac{1}{2d}\left(z^2 - \frac{a^2}{2}\right), \quad \lambda_j = \frac{j\pi}{d} \tag{3.32}$$

Now, find Fourier coefficients α_j. Integrate equation (3.32) from 0 to d with respect to z to calculate α_0:

$$\alpha_0 = \left(\sum_{\ell=0}^{\infty} A_\ell R_\ell(k_\ell a) E_{0\ell}\right) - \left(\frac{d}{3} - \frac{a^2}{2d}\right) \tag{3.33}$$

Multiply (3.32) with $\cos(\lambda_j z)$ and integrate from 0 to d with respect to z to calculate α_j:

$$\alpha_j = \frac{2}{d}\left[\int_0^d \phi^{(e)}(a,z)\cos(\lambda_j z)dz - \frac{1}{2d}\int_0^d \left(z^2 - \frac{a^2}{2}\right)\cos(\lambda_j z)dz\right]$$

After calculations of the integrals,

$$\alpha_j = \left(\sum_{\ell=0}^{\infty} A_\ell R_\ell(k_\ell a) E_{j\ell}\right) - (-1)^j \frac{2d}{j^2\pi^2} \quad j = 1, 2, ... \tag{3.34}$$

We can rewrite infinite system for α_j:

$$\alpha_j = \left(\sum_{\ell=0}^{\infty} A_\ell R_\ell(k_\ell a) E_{j\ell}\right) - \alpha_j^* \quad j = 0, 1, ... \tag{3.35}$$

where

$$\alpha_j^* = \begin{cases} \frac{d}{3} - \frac{a^2}{2d}, & j = 0 \\ (-1)^j \frac{2d}{j^2\pi^2}, & j \geq 1 \end{cases} \tag{3.36}$$

The coefficient systems of α_j and A_ℓ are related. We can substitude one system to the other to eliminate the unknowns. We need the potential $\phi^{(i)}$ for the calculation of added mass and damping coefficients in heave motion. So, substitude equation (3.28) into (3.35) and we get:

$$\alpha_j = \sum_{\ell=0}^{\infty} \frac{\left(A_\ell^* + \sum_{s=0}^{\infty} \alpha_s S_s E_{s\ell}\right) R_\ell E_{j\ell}}{k_\ell R_\ell'} - \alpha_j^*, \quad j = 0, 1, \ldots \tag{3.37}$$

$$\alpha_j - \sum_{\ell=0}^{\infty} R_\ell E_{j\ell} \frac{\sum_{s=0}^{\infty} \alpha_s S_s E_{s\ell}}{k_\ell R'_\ell} = \sum_{\ell=0}^{\infty} \frac{A^*_\ell R_\ell E_{j\ell}}{k_\ell R'_\ell} - \alpha^*_j, \quad j = 0, 1, \ldots$$

$$\alpha_j - \sum_{s=0}^{\infty} \alpha_s S_s \sum_{\ell=0}^{\infty} \frac{R_\ell E_{j\ell} E_{s\ell}}{k_\ell R'_\ell} = g_j, \quad j = 0, 1, \ldots$$

We can replace α_j with the identity

$$\alpha_j = \sum_{s=0}^{\infty} \delta_{js} \alpha_s, \quad j = 0, 1, \ldots$$

where δ_{js} is the Kronecker delta. Hence,

$$\sum_{s=0}^{\infty} [\delta_{js} - e_{js}] \alpha_s = g_j, \quad j = 0, 1, \ldots \tag{3.38}$$

where

$$e_{js} = \left[\sum_{\ell=0}^{\infty} \frac{R_\ell E_{j\ell} E_{s\ell}}{k_\ell R'_\ell} \right] S_s \tag{3.39}$$

$$g_j = \sum_{\ell=0}^{\infty} \frac{A^*_\ell R_\ell E_{j\ell}}{k_\ell R'_\ell} - \alpha^*_j \tag{3.40}$$

The system of equations can be represented in matrix form:

$$\underbrace{\begin{bmatrix} 1 & -e_{01} & \ldots & -e_{0n} \\ 0 & 1 - e_{11} & \ldots & -e_{1n} \\ \vdots & \vdots & \vdots & \vdots \\ 0 & -e_{n1} & \ldots & 1 - e_{nn} \end{bmatrix}}_{\mathbf{A}} \underbrace{\begin{bmatrix} \alpha_0 \\ \alpha_1 \\ \vdots \\ \alpha_n \end{bmatrix}}_{\mathbf{x}} = \underbrace{\begin{bmatrix} g_0 \\ g_1 \\ \vdots \\ g_n \end{bmatrix}}_{\mathbf{b}}$$

$$\alpha_0 = g_0 + \sum_{i=1}^{n} e_{0i} \alpha_i \tag{3.41}$$

First, the matrix system is solved for α_j, $j = 1, 2, ...$ since S_0 vanishes. Then, we can calculate α_0 in case of $j = 0$ in the equation (3.41) and unknown coefficients A_ℓ in the equation (3.28). Mostly, 12 equations are enough. In Appendix D, behaviour of α_j and A_ℓ for variying number of equations are given.

3.2. Added Mass and Damping Coefficients

The velocity potential $\Phi(r, \theta, z, t)$ for a vertical cylinder with circular cross-section is defined as follows:

$$\Phi(r, \theta, z, t) = \bar{h} Re[-i\sigma\bar{\xi}_3 e^{-i\sigma t}\phi(r, z)] \tag{3.42}$$

The force can be determined by integrating the fluid pressure, $p = -\rho\frac{\partial\Phi}{\partial t}$, over the wetted surface of the cylinder S. The real and imaginary parts of F_z are defined heave added mass and damping coefficients (Newman (2018)). The added mass coefficient represents the force component proportional to the acceleration and the damping coefficient gives a force proportional to the body velocity.

$$F_z = \iint_S p\mathbf{n}dS = -\rho \iint_S \frac{\partial\Phi}{\partial t}.1dS$$

Note that, $n_z = 1$ and $\bar{r}/\bar{h} = r$.

$$dS = \bar{r}d\bar{r}d\theta$$
$$dS = \bar{h}^2 r dr d\theta$$

$$F_z = +\rho \int_0^{2\pi}\int_0^a \bar{h}^3\sigma^2\bar{\xi}_3 e^{-i\sigma t}\phi(r, z) r dr d\theta \tag{3.43}$$

$$F_z = \rho\bar{h}^3\sigma^2\bar{\xi}_3 \int_0^{2\pi}\int_0^a \phi(r, z).1 r dr d\theta \quad \text{since} \quad max(e^{-i\sigma t}) = 1 \tag{3.44}$$

Body boundary condition $\frac{\partial\phi^{(i)}}{\partial z} = 1$ at $z = d$, $r \leq a$ can be substituted into equation (3.42).

$$F_z = \rho\bar{h}^3\sigma^2\bar{\xi}_3 \int_0^{2\pi}\int_0^a \phi^{(i)}(r, d)\frac{\partial\phi^{(i)}(r, d)}{\partial z} r dr d\theta \tag{3.45}$$

$$F_z = \rho\bar{h}^3\sigma^2\bar{\xi}_3 \int_0^{2\pi}\int_0^a \left(\frac{1}{2d}\left(z^2 - \frac{r^2}{2}\right) + \frac{\alpha_0}{2} + \sum_{j=1}^{\infty}\alpha_j\frac{I_0(\lambda_j r)}{I_0(\lambda_j a)}\cos(\lambda_j d)\right) r dr d\theta \tag{3.46}$$

where $\lambda_j = \frac{j\pi}{d}$, $j \geq 1$. Integration of modified Bessel function of the first kind I_0 is given in Appendix B.

$$F_z = \rho\bar{h}^3\sigma^2\bar{\xi}_3 2\pi\left(\frac{da^2}{4} - \frac{a^4}{16d} + \frac{\alpha_0 a^2}{4} + \sum_{j=1}^{\infty}(-1)^j\alpha_j\frac{aI_1(\lambda_j a)}{\lambda_j I_0(\lambda_j a)}\right) \tag{3.47}$$

The non-dimensional added mass and damping coefficients in the paper Yeung (1981) are given by the relation

$$\mu_{33} + i\lambda_{33} = \frac{F_z}{\sigma^2\bar{\xi}_3\rho\pi\bar{a}^3} \tag{3.48}$$

$$\mu_{33} + i\lambda_{33} = \frac{d}{2a} - \frac{a}{8d} + \frac{\alpha_0}{2a} + \frac{4d}{a^2}\sum_{j=1}^{\infty}\alpha_j(-1)^j\frac{S_j}{(j\pi)^2} \tag{3.49}$$

where

$$S_j = \frac{j\pi}{2}\frac{I_0'(\lambda_j a)}{I_0(\lambda_j a)}, \quad \lambda_j = \frac{j\pi}{d} \tag{3.50}$$

3.3. Computational Results

The process start with calculation of v for different values of k_0 which satisfies $k_0 tanh(k_0) = v$. If v is known, then we can find k_ℓ from the relation $k_\ell tan(k_\ell) = -v$ by using the Newton-Raphson method. The first four terms of $k_\ell a$ are presented in the Table 3.1 for various $k_0 a$ where $a = 1.0$. First five coefficiens α_j, A_ℓ and the result of added mass and damping for different number of equations is shown in Appendix D.

Table 3.1. Solutions of $k_\ell a$ for various $k_0 a$ and $a = 1.0$

	$k_0a = 0.5$	$k_0a = 1.0$	$k_0a = 1.5$	$k_0a = 2.0$	$k_0a = 2.5$	$k_0a = 3.0$
k_1a	3.0664	2.8834	2.6714	2.4809	2.3271	2.2075
k_2a	6.2462	6.1602	6.0629	5.9708	5.8864	5.8085
k_3a	9.4002	9.3434	9.2795	9.2186	9.1618	9.1081
k_4a	12.5480	12.5055	12.4578	12.4123	12.3695	12.3288

Figure 3.2 and 3.3 show the non-dimensional added mass and damping for different non-dimensionalized radius a with parameter d. Added mass coefficients for a=5.0 and a=1.0 are close. Damping coefficients are approaching to zero and added mass coefficients are approaching to a constant (approximately $k_0 a > 1$) for all the cases. Added mass coefficients decrease, whenever d increases. Also, damping coefficients increase whenever d increases (whenever $k_0 a$ approaches to zero). However, at the same depth, damping was weakly affected. Note that, these numerical results are important for the asymptotic solutions of the present thesis. Because of the zeroth-order system of asymptotic approach is the same as the circular cylinder case.

(a)

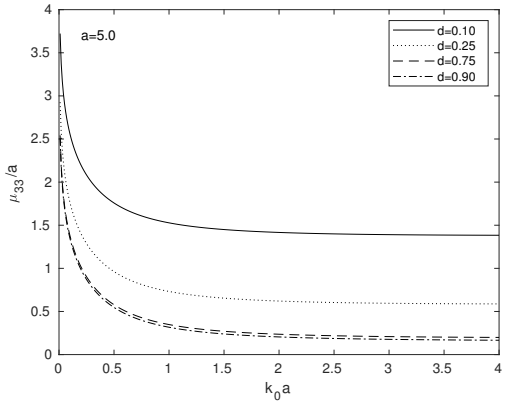

(b)

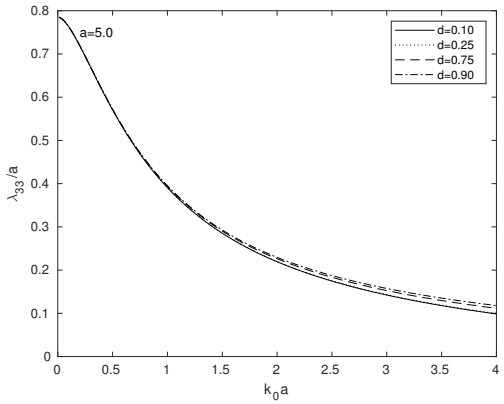

(c)

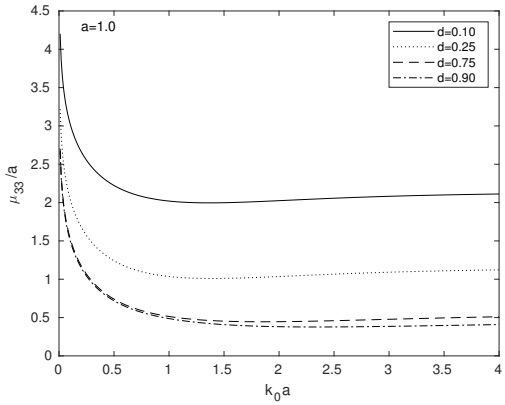

(d)

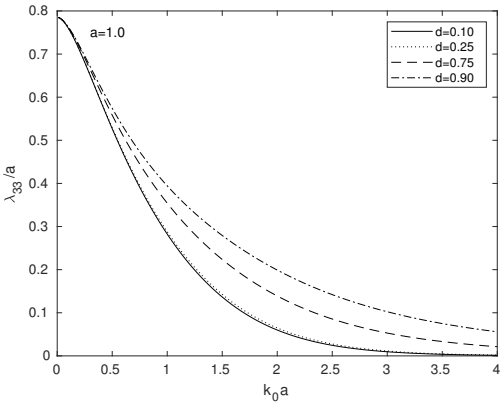

Figure 3.2. Added mass and damping coefficients for heaving motion: $a = 5.0$ and $a = 1.0$

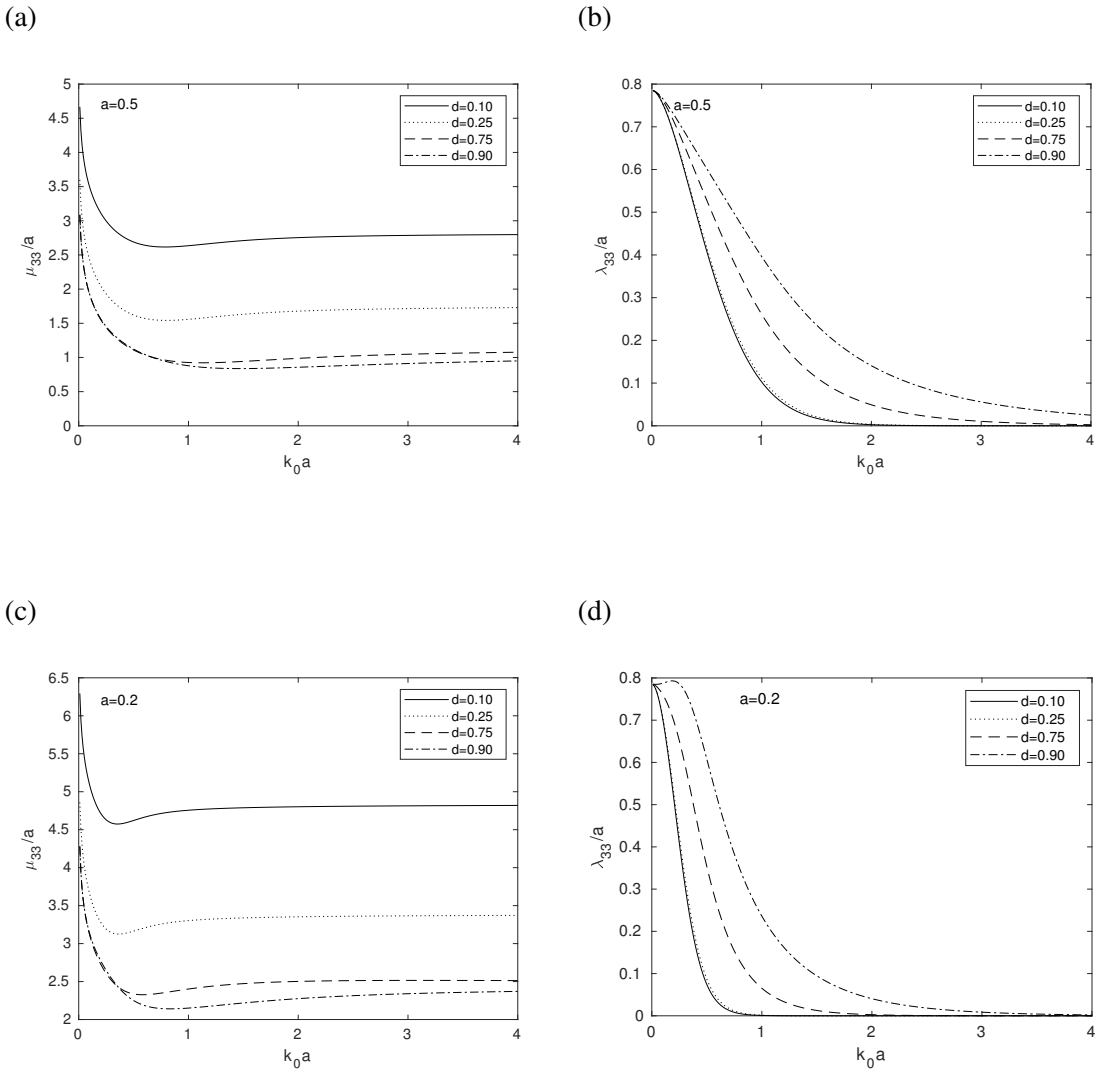

Figure 3.3. Added mass and damping coefficients for heaving motion: $a = 0.5$ and $a = 0.2$

CHAPTER 4

WAVE RADIATION IN HEAVING MOTION FROM A VERTICAL CYLINDER OF ARBITRARY CROSS SECTION

The wave radiation problem in heaving motion by a vertical cylinder of an arbitrary cross-section is solved by an asymptotic approach. We can note that the asymptotic solution of wave diffraction from a bottom-mounted vertical cylinder with different cross-sections was presented by Dişibüyük et al. (2017) using the fifth-order approximation which has good agreement with numerical and experimental results. The asymptotic method of this thesis was suggested by Dişibüyük et al. (2017). The non-dimensional maximum deviation of the cylinder cross-section from a circular one is assumed the small parameter of the problem by Dişibüyük et al. (2017). In this chapter, we studied a third-order asymptotic solution. Unknown coefficients of interior and exterior potentials are solved by using Fourier series of the shape function at each order of approximation. The advantage of the method is that the boundary conditions can be solved for different cross-sections by using the Fourier coefficients. The asymptotic approach is applied for cylinders with different cross-sections such as elliptic, quasi-elliptic, square, and cosine cross-section. The computatonal results are compared with other studies.

Yu et al. (2019) extended their studies to cylinders with a different cross-section and, they suggested a semi-analytical solution to this problem. The method for finding unknown hydrodynamic coefficients by matching velocities in the common region was the same as in other studies. However, the radius function was defined in cylindrical coordinates and the boundary conditions are solved by writing the radius function into the Fourier series. Added mass and damping were calculated for cylinders with circular, cosine, elliptical, and quasi-elliptical cross-sections where same depth and cross-sectional area is assumed. Added mass and damping coefficients for the quasi-elliptic type were calculated in different drafts. The results were used to compare with the asymptotic approaches obtained in this thesis.

4.1. Mathematical Formulation

We deal with a vertical cylinder with arbitrary cross-section of finite draft in finite depth water. Seabed is horizontal and fixed. The bottom surface of the water is Oxy plane, (r, θ) is polar coordinates, and z-axis point upwards. Gravitational acceleration g is in z direction. The floating body oscillates time-harmonically along the z-axis. The cylinder extends from d to the free surface (Figure 4.1). The radius of the cross-section is described by the equation $r = R[1 + \varepsilon f(\theta)]$ where R is the mean radius of the cylinder, ε be the small non-dimensional parameter of the problem and $f(\theta)$ is the smooth, bounded and periodic, $f(\theta) = f(\theta + 2\pi)$, function which is the deviation of the shape of the cross-section from the circular one (Dişibüyük et al. (2017)).

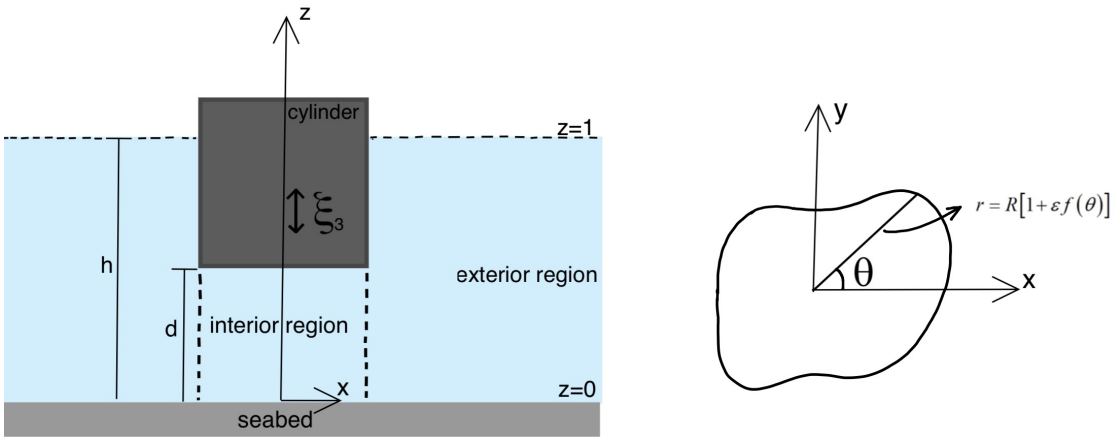

Figure 4.1. Coordinate system and notations

If inviscid fluid flow is assumed, we can define the velocity potential as follows:

$$\Phi(r, \theta, z, t) = \bar{h} Re[-i\sigma\xi_3 e^{-i\sigma t}\phi(r, \theta, z)] \tag{4.1}$$

where σ is the angular frequency, ξ_3 the heave amplitude, and $i = \sqrt{-1}$. The potential $\phi(r, \theta, z)$ satisfy the following equations:

$$\nabla^2\phi = 0 \tag{4.2}$$

$$\frac{\partial\phi}{\partial z} - \nu\phi = 0 \quad \text{on } z = 1, \quad \nu = \frac{\sigma^2}{g}\bar{h} \tag{4.3}$$

$$\frac{\partial \phi}{\partial z} = 0 \quad \text{at z=0} \tag{4.4}$$

$$\frac{\partial \phi}{\partial z} = 1 \quad \text{on } z = d, \quad 0 \le r \le R[1 + \varepsilon f(\theta)] \tag{4.5}$$

$$\frac{\partial \phi}{\partial n} = \nabla \phi \cdot \mathbf{n} = 0 \quad \text{on } r = R[1 + \varepsilon f(\theta)], \quad d \le z \le 1 \tag{4.6}$$

$$\phi \to 0 \quad \text{as} \quad r \to \infty \tag{4.7}$$

where the normal vector $\mathbf{n}$ is the pointing out. The potential ϕ is finite at $r = 0$.

4.2. Vertical Cylinder with Nearly Circular Cross Section

If we expand equation (4.6), we get

$$\nabla \phi = \left(\frac{\partial \phi}{\partial r}, \frac{1}{r}\frac{\partial \phi}{\partial \theta}, \frac{\partial \phi}{\partial z}\right) \tag{4.8}$$

$$\mathbf{n} = \frac{\nabla f}{|\nabla f|}, \quad f = r - R[1 + \varepsilon f(\theta)] \tag{4.9}$$

$$\mathbf{n} = \frac{1}{\sqrt{1 + \frac{[R\varepsilon f'(\theta)]^2}{r^2}}} \left(1, \frac{-R\varepsilon f'(\theta)}{r}\right) \tag{4.10}$$

$$\nabla \phi \cdot \mathbf{n} = \frac{1}{\sqrt{1 + \frac{[R\varepsilon f'(\theta)]^2}{R^2[1+\varepsilon f(\theta)]^2}}} \left(\frac{\partial \phi}{\partial r} - \frac{\varepsilon f'(\theta)}{R[1 + \varepsilon f(\theta)]^2}\frac{\partial \phi}{\partial \theta}\right) = 0 \tag{4.11}$$

on $r = R[1 + \varepsilon f(\theta)]$.

As in the cylinder with circular cross-section, we must divide the region into two parts: interior and exterior. Then we will write the asymptotic expansions of the boundary conditions provided by the interior and exterior potentials and calculate the unknown coefficients while the leading order $\varepsilon \to 0$.

4.2.1. Interior and Exterior Solutions

The interior solution $\phi^{(i)}(r, \theta, z)$ satisfy the equations (4.2), (4.4), (4.5) and the exterior solution $\phi^{(e)}(r, \theta, z)$ satisfy the equations (4.2), (4.3), (4.4), (4.6) and (4.7). The

potentials are given by the asymptotic expansions up to $O(\varepsilon^4)$ for a small parameter ε.

$$\phi^{(i)}(r,\theta,z) = \phi_0^{(i)}(r,\theta,z) + \varepsilon\phi_1^{(i)}(r,\theta,z) + \varepsilon^2\phi_2^{(i)}(r,\theta,z) + \varepsilon^3\phi_3^{(i)}(r,\theta,z) + O(\varepsilon^4) \tag{4.12}$$

$$\phi^{(e)}(r,\theta,z) = \phi_0^{(e)}(r,\theta,z) + \varepsilon\phi_1^{(e)}(r,\theta,z) + \varepsilon^2\phi_2^{(e)}(r,\theta,z) + \varepsilon^3\phi_3^{(e)}(r,\theta,z) + O(\varepsilon^4) \tag{4.13}$$

The potentials $\phi^{(i)}(r,\theta,z)$ and $\phi^{(e)}(r,\theta,z)$ are matched at $r = R[1 + \varepsilon f(\theta)]$ and $0 \le z \le d$ by the continuity of pressure and the continuity of normal velocity between interior and exterior regions.

$$\phi^{(e)}(R[1+\varepsilon f(\theta)],\theta,z) = \phi^{(i)}(R[1+\varepsilon f(\theta)],\theta,z) \tag{4.14}$$

$$\left.\frac{\partial\phi^{(e)}}{\partial n}\right|_{r=R[1+\varepsilon f(\theta)]} = \left.\frac{\partial\phi^{(i)}}{\partial n}\right|_{r=R[1+\varepsilon f(\theta)]} \tag{4.15}$$

The partial derivatives $\partial\phi/\partial\theta$ and $\partial\phi/\partial r$ on the $R[1 + \varepsilon f(\theta)]$ are approximated by their Taylor series up to $O(\varepsilon^4)$ at $r = R$. Then substitute asymptotic expansions of $\phi^{(i)}$ and $\phi^{(e)}$ at $r = R$ into conditions (4.11), (4.14) and (4.15).

The condition (4.11) gives:

$$\begin{aligned}
&\phi_{0,r}^{(e)} + \varepsilon\left[\phi_{1,r}^{(e)} + Rf(\theta)\phi_{0,rr}^{(e)} - \frac{f'(\theta)}{R}\phi_{0,\theta}^{(e)}\right] \\
&\quad + \varepsilon^2\left[\phi_{2,r}^{(e)} + Rf(\theta)\phi_{1,rr}^{(e)} - \frac{f'(\theta)}{R}\phi_{1,\theta}^{(e)} + \frac{R^2f^2(\theta)}{2}\phi_{0,rrr}^{(e)} + \frac{2f(\theta)f'(\theta)}{R}\phi_{0,\theta}^{(e)} - f(\theta)f'(\theta)\phi_{0,r\theta}^{(e)}\right] \\
&\quad + \varepsilon^3\left[\begin{array}{l}\phi_{3,r}^{(e)} + \frac{1}{6}R^3f(\theta)^3\phi_{0,rrrr}^{(e)} + \frac{1}{2}R^2f(\theta)^2\phi_{1,rrr}^{(e)} + 2f(\theta)^2f'(\theta)\phi_{0,r\theta}^{(e)} - \frac{1}{2}Rf(\theta)^2f'(\theta)\phi_{0,rr\theta}^{(e)} \\ -\frac{3f(\theta)^2f'(\theta)\phi_{0,\theta}^{(e)}}{R} + \frac{2f(\theta)f'(\theta)\phi_{1,\theta}^{(e)}}{R} - f(\theta)f'(\theta)\phi_{1,r\theta}^{(e)} - \frac{f'(\theta)\phi_{2,\theta}^{(e)}}{R} + Rf(\theta)\phi_{2,rr}^{(e)}\end{array}\right] \\
&\quad = \mathrm{O}(\varepsilon^4) \quad \text{where} \quad r = R, \quad d \le z \le 1.
\end{aligned}$$

The condition (4.14) gives:

$$\begin{aligned}
&\phi_0^{(e)}+\varepsilon\left[\phi_1^{(e)}+Rf(\theta)\phi_{0,r}^{(e)}\right]+\varepsilon^2\left[\phi_2^{(e)}+Rf(\theta)\phi_{1,r}^{(e)}+\frac{R^2f^2(\theta)}{2}\phi_{0,rr}^{(e)}\right]\\
&\quad+\varepsilon^3\left[\phi_3^{(e)}+\frac{1}{6}R^3f(\theta)^3\phi_{0,rrr}^{(e)}+\frac{1}{2}R^2f(\theta)^2\phi_{1,rr}^{(e)}+Rf(\theta)\phi_{2,r}^{(e)}\right]\\
&=\phi_0^{(i)}+\varepsilon\left[\phi_1^{(i)}+Rf(\theta)\phi_{0,r}^{(i)}\right]+\varepsilon^2\left[\phi_2^{(i)}+Rf(\theta)\phi_{1,r}^{(i)}+\frac{R^2f^2(\theta)}{2}\phi_{0,rr}^{(i)}\right]\\
&\quad+\varepsilon^3\left[\phi_3^{(i)}+\frac{1}{6}R^3f(\theta)^3\phi_{0,rrr}^{(i)}+\frac{1}{2}R^2f(\theta)^2\phi_{1,rr}^{(i)}+Rf(\theta)\phi_{2,r}^{(i)}\right]\\
&\quad+\mathrm{O}(\varepsilon^4)\quad\text{where}\quad r=R,\quad 0\le z\le d.
\end{aligned}$$

The condition (4.15) gives:

$$\begin{aligned}
&\phi_{0,r}^{(e)}+\varepsilon\left[\phi_{1,r}^{(e)}+Rf(\theta)\phi_{0,rr}^{(e)}-\frac{f'(\theta)}{R}\phi_{0,\theta}^{(e)}\right]\\
&\quad+\varepsilon^2\left[\phi_{2,r}^{(e)}+Rf(\theta)\phi_{1,rr}^{(e)}-\frac{f'(\theta)}{R}\phi_{1,\theta}^{(e)}+\frac{R^2f^2(\theta)}{2}\phi_{0,rrr}^{(e)}+\frac{2f(\theta)f'(\theta)}{R}\phi_{0,\theta}^{(e)}-f(\theta)f'(\theta)\phi_{0,r\theta}^{(e)}\right]\\
&\quad+\varepsilon^3\left[\begin{array}{l}\phi_{3,r}^{(e)}+\frac{1}{6}R^3f(\theta)^3\phi_{0,rrrr}^{(e)}+\frac{1}{2}R^2f(\theta)^2\phi_{1,rrr}^{(e)}+2f(\theta)^2f'(\theta)\phi_{0,r\theta}^{(e)}-\frac{1}{2}Rf(\theta)^2f'(\theta)\phi_{0,rr\theta}^{(e)}\\-\frac{3f(\theta)^2f'(\theta)\phi_{0,\theta}^{(e)}}{R}+\frac{2f(\theta)f'(\theta)\phi_{1,\theta}^{(e)}}{R}-f(\theta)f'(\theta)\phi_{1,r\theta}^{(e)}-\frac{f'(\theta)\phi_{2,\theta}^{(e)}}{R}+Rf(\theta)\phi_{2,rr}^{(e)}\end{array}\right]\\
&=\phi_{0,r}^{(i)}+\varepsilon\left[\phi_{1,r}^{(i)}+Rf(\theta)\phi_{0,rr}^{(i)}-\frac{f'(\theta)}{R}\phi_{0,\theta}^{(i)}\right]\\
&\quad+\varepsilon^2\left[\phi_{2,r}^{(i)}+Rf(\theta)\phi_{1,rr}^{(i)}-\frac{f'(\theta)}{R}\phi_{1,\theta}^{(i)}+\frac{R^2f^2(\theta)}{2}\phi_{0,rrr}^{(i)}+\frac{2f(\theta)f'(\theta)}{R}\phi_{0,\theta}^{(i)}-f(\theta)f'(\theta)\phi_{0,r\theta}^{(i)}\right]\\
&\quad+\varepsilon^3\left[\begin{array}{l}\phi_{3,r}^{(i)}+\frac{1}{6}R^3f(\theta)^3\phi_{0,rrrr}^{(i)}+\frac{1}{2}R^2f(\theta)^2\phi_{1,rrr}^{(i)}+2f(\theta)^2f'(\theta)\phi_{0,r\theta}^{(i)}-\frac{1}{2}Rf(\theta)^2f'(\theta)\phi_{0,rr\theta}^{(i)}\\-\frac{3f(\theta)^2f'(\theta)\phi_{0,\theta}^{(i)}}{R}+\frac{2f(\theta)f'(\theta)\phi_{1,\theta}^{(i)}}{R}-f(\theta)f'(\theta)\phi_{1,r\theta}^{(i)}-\frac{f'(\theta)\phi_{2,\theta}^{(i)}}{R}+Rf(\theta)\phi_{2,rr}^{(i)}\end{array}\right]\\
&\quad+\mathrm{O}(\varepsilon^4)\quad\text{where}\quad r=R,\quad 0\le z\le d.
\end{aligned}$$

At the leading order as $\varepsilon \to 0$,

$$\phi_{0,r}^{(e)}(R,\theta,z) = \begin{cases} 0, & d \le z \le 1 \\ \phi_{0,r}^{(i)}, & 0 \le z \le d \end{cases} \tag{4.16}$$

$$\phi_0^{(i)}(R,\theta,z) = \phi_0^{(e)}(R,\theta,z), \quad 0 \le z \le d \tag{4.17}$$

We can say that $\phi_0^{(i)}$ and $\phi_0^{(e)}$ are the velocity potentials of heave motion for the circular cylinder. The problem for circular cylinder, $r = R$, is shown in Chapter 3.

$$\phi_0^{(i)} = \frac{1}{2d}\left(z^2 - \frac{r^2}{2}\right) + \frac{\alpha_0}{2} + \sum_{j=1}^{\infty} \alpha_n \frac{I_0(\lambda_j r)}{I_0(\lambda_j R)} cos(\lambda_j z), \quad \lambda_j = \frac{j\pi}{d} \tag{4.18}$$

$$\phi_0^{(e)} = A_0 H_0^{(1)}(k_0 r) Z_0(k_0 z) + \sum_{l=1}^{\infty} A_l K_0(k_l r) Z_l(k_l z) \tag{4.19}$$

where $Z_0 = cosh(k_0 z)/N_0^{1/2}$ and $Z_l = cos(k_l z)/N_l^{1/2}$ since Z_ℓ is orthonormal set in [0,1] (see Appendix A). From the free surface conditions, k_0 satisfies $k_0 tanh(k_0) = \nu$ and k_l satisfies $k_l tan(k_l) = -\nu$.

At the first order, we get

$$\phi_{1,r}^{(e)}(R,\theta,z) = \begin{cases} -Rf(\theta)\phi_{0,rr}^{(e)} + \frac{f'(\theta)\phi_{0,\theta}^{(e)}}{R}, & d \le z \le 1 \\ \\ \phi_{1,r}^{(i)} - Rf(\theta)\phi_{0,rr}^{(e)} + \frac{f'(\theta)\phi_{0,\theta}^{(e)}}{R} - \frac{f'(\theta)\phi_{0,\theta}^{(i)}}{R} + Rf(\theta)\phi_{0,rr}^{(i)}, & 0 \le z \le d \end{cases} \tag{4.20}$$

$$\phi_1^{(i)}(R,\theta,z) = \phi_1^{(e)} + Rf(\theta)\phi_{0,r}^{(e)} - Rf(\theta)\phi_{0,r}^{(i)}, \quad 0 \le z \le d \tag{4.21}$$

At the second and higher orders, we get

$$\phi_{2,r}^{(e)}(R,\theta,z)=\begin{cases}-\frac{1}{2}R^2f(\theta)^2\phi_{0,rrr}^{(e)}-\frac{2f(\theta)f'(\theta)\phi_{0,\theta}^{(e)}}{R}+f(\theta)f'(\theta)\phi_{0,r\theta}^{(e)}\\+\frac{f'(\theta)\phi_{1,\theta}^{(e)}}{R}-Rf(\theta)\phi_{1,rr}^{(e)}, & d\le z\le 1\\ \\ \phi_{2,r}^{(i)}-\frac{1}{2}R^2f(\theta)^2\phi_{0,rrr}^{(e)}-\frac{2f(\theta)f'(\theta)\phi_{0,\theta}^{(e)}}{R}+f(\theta)f'(\theta)\phi_{0,r\theta}^{(e)}\\+Rf(\theta)\phi_{1,rr}^{(e)}+\frac{1}{2}R^2f(\theta)^2\phi_{0,rrr}^{(i)}+\frac{2f(\theta)f'(\theta)\phi_{0,\theta}^{(i)}}{R}\\-f(\theta)f'(\theta)\phi_{0,r\theta}^{(i)}-\frac{f'(\theta)\phi_{1,\theta}^{(i)}}{R}+Rf(\theta)\phi_{1,rr}^{(i)}, & 0\le z\le d\end{cases}\tag{4.22}$$

$$\begin{aligned}\phi_2^{(i)}(R,\theta,z)=&\phi_2^{(e)}+\left(\frac{1}{2}R^2f(\theta)^2\phi_{0,rr}^{(e)}+Rf(\theta)\phi_{1,r}^{(e)}\right)\\&-\left(\frac{1}{2}R^2f(\theta)^2\phi_{0,rr}^{(i)}+Rf(\theta)\phi_{1,r}^{(i)}\right),\quad 0\le z\le d\end{aligned}\tag{4.23}$$

$$\phi_{3,r}^{(e)}(R,\theta,z)=\begin{cases}-\frac{1}{6}R^3f(\theta)^3\phi_{0,rrrr}^{(e)}-\frac{1}{2}R^2f(\theta)^2\phi_{1,rrr}^{(e)}-2f(\theta)^2f'(\theta)\phi_{0,r\theta}^{(e)}\\+\frac{1}{2}Rf(\theta)^2f'(\theta)\phi_{0,rr\theta}^{(e)}+\frac{3f(\theta)^2f'(\theta)\phi_{0,\theta}^{(e)}}{R}-\frac{2f(\theta)f'(\theta)\phi_{1,\theta}^{(e)}}{R}\\+f(\theta)f'(\theta)\phi_{1,r\theta}^{(e)}+\frac{f'(\theta)\phi_{2,\theta}^{(e)}}{R}-Rf(\theta)\phi_{2,rr}^{(e)}, & d\le z\le 1\\ \\ \phi_{3,r}^{(i)}-\frac{1}{6}R^3f(\theta)^3\phi_{0,rrrr}^{(e)}-\frac{1}{2}R^2f(\theta)^2\phi_{1,rrr}^{(e)}\\-2f(\theta)^2f'(\theta)\phi_{0,r\theta}^{(e)}+\frac{1}{2}Rf(\theta)^2f'(\theta)\phi_{0,rr\theta}^{(e)}+\frac{3f(\theta)^2f'(\theta)\phi_{0,\theta}^{(e)}}{R}\\-\frac{2f(\theta)f'(\theta)\phi_{1,\theta}^{(e)}}{R}+f(\theta)f'(\theta)\phi_{1,r\theta}^{(e)}+\frac{f'(\theta)\phi_{2,\theta}^{(e)}}{R}\\-Rf(\theta)\phi_{2,rr}^{(e)}+\frac{1}{6}R^3\phi_{0,rrrr}^{(i)}f(\theta)^3+2f'(\theta)\phi_{0,r\theta}^{(i)}f(\theta)^2\\-\frac{1}{2}Rf'(\theta)\phi_{0,rr\theta}^{(i)}f(\theta)^2+\frac{1}{2}R^2\phi_{1,rrr}^{(i)}f(\theta)^2-\frac{3f'(\theta)\phi_{0,\theta}^{(i)}f(\theta)^2}{R}\\+\frac{2f'(\theta)\phi_{1,\theta}^{(i)}f(\theta)}{R}-f'(\theta)\phi_{1,r\theta}^{(i)}f(\theta)+R\phi_{2,rr}^{(i)}f(\theta)\\-\frac{f'(\theta)\phi_{2,\theta}^{(i)}}{R}, & 0\le z\le d\end{cases}\tag{4.24}$$

$$\begin{aligned}\phi_3^{(i)}(R,\theta,z)=&\phi_3^{(e)}+\frac{1}{6}R^3f(\theta)^3\phi_{0,rrr}^{(e)}+\frac{1}{2}R^2f(\theta)^2\phi_{1,rr}^{(e)}+Rf(\theta)\phi_{2,r}^{(e)}\\&-\frac{1}{6}R^3f(\theta)^3\phi_{0,rrr}^{(i)}-\frac{1}{2}R^2f(\theta)^2\phi_{1,rr}^{(i)}+Rf(\theta)\phi_{2,r}^{(i)},\quad 0\le z\le d\end{aligned}\tag{4.25}$$

where the portentials $\phi_n^{(i)}(r,\theta,z)$, $\phi_n^{(e)}(r,\theta,z)$ and their derivatives calculated at $r = R$. The subnotation after comma represents the partial derivative of the function such as $\phi_{0,r}^{(i)} = \frac{\partial \phi_0^{(i)}}{\partial r}$.

The potentials $\phi_n^{(e)}$ and $\phi_n^{(i)}$, n=1,2,3 can be written in terms of Fourier coefficients as

$$\phi_n^{(e)} = \sum_{m=0}^{\infty}[A_{n,m,0}cos(m\theta) + B_{n,m,0}sin(m\theta)]H_m^{(1)}(k_0 r)Z_0(k_0 z) + \sum_{l=1}^{\infty}\sum_{m=0}^{\infty}\left[A_{n,m,l}cos(m\theta) + B_{n,m,l}sin(m\theta)\right]K_m(k_l r)Z_l(k_l z) \tag{4.26}$$

$$\phi_n^{(i)} = \sum_{j=0}^{\infty}\sum_{m=0}^{\infty}[C_{n,m,j}cos(m\theta) + D_{n,m,j}sin(m\theta)]\frac{I_m(\lambda_j r)}{I_m(\lambda_j R)}cos(\lambda_j z) \tag{4.27}$$

The coefficients $A_{n,m,l}$, $B_{n,m,l}$, $C_{n,m,j}$ and $D_{n,m,j}$ are unknowns at the moment. They are found by using the boundary conditions (4.20)-(4.25). If the Fourier coefficients of $f(\theta)$ are known, we have

$$f(\theta) = \frac{f_0^{(c)}}{2} + \sum_{m=1}^{\infty} f_m^{(c)}\cos(m\theta) + f_m^{(s)}\sin(m\theta) \tag{4.28}$$

The derivatives of potenatials $\phi_0^{(i)}(r,z)$, $\phi_0^{(e)}(r,z)$ at $r = R$ (see equations (4.18) and (4.19)) and the Fourier series of the function $f(\theta)$ are substituted into (4.20) and (4.21) to find the solution of $\phi_1^{(i)}(r,\theta,z)$ and $\phi_1^{(e)}(r,\theta,z)$. First, we should eliminate the z dependence in system of equations by using the function Z_ℓ is normalized orthogonal set in [0,1] (see Appendix A). As in the circular cylinder, the coefficients in the interior and exterior potentials are dependent. So, we have to use these matching conditions to eliminate the coefficients A and B to find the coefficients C and D. In Subsection 4.3, the potentials $\phi_n^{(i)}$, $n = 0, 1, 2, 3$ is used to find force in z direction. Similarly, higher-order problems for $\phi_2^{(i)}$, $\phi_2^{(e)}$, $\phi_3^{(i)}$, and $\phi_3^{(e)}$ can be solved. The identity for product of Fourier series are given in Appendix C is required.

In case the shape function depend on the small parameter ε ($r = R[1 + \varepsilon f(\theta, \varepsilon)]$), $f(\theta, \varepsilon)$ can be approximated as

$$f(\theta, \varepsilon) = f_0(\theta) + \varepsilon f_1(\theta) + \varepsilon^2 f_2(\theta) + \varepsilon^3 f_3(\theta) + O(\varepsilon^4) \tag{4.29}$$

$$\phi_{0,r}^{(e)}(R, \theta, z) = \begin{cases} 0, & d \le z \le 1 \\ \phi_{0,r}^{(i)}, & 0 \le z \le d \end{cases} \tag{4.30}$$

$$\phi_0^{(i)}(R, \theta, z) = \phi_0^{(e)}(R, \theta, z), \quad 0 \le z \le d \tag{4.31}$$

$$\phi_{1,r}^{(e)}(R, \theta, z) = \begin{cases} -Rf_0(\theta)\phi_{0,rr}^{(e)} + \frac{f_0'(\theta)\phi_{0,\theta}^{(e)}}{R}, & d \le z \le 1 \\ \phi_{1,r}^{(i)} - Rf_0(\theta)\phi_{0,rr}^{(e)} + \frac{f_0'(\theta)\phi_{0,\theta}^{(e)}}{R} - \frac{f_0'(\theta)\phi_{0,\theta}^{(i)}}{R} + Rf_0(\theta)\phi_{0,rr}^{(i)}, & 0 \le z \le d \end{cases} \tag{4.32}$$

$$\phi_1^{(i)}(R, \theta, z) = \phi_1^{(e)} + Rf_0(\theta)\phi_{0,r}^{(e)} - Rf_0(\theta)\phi_{0,r}^{(i)}, \quad 0 \le z \le d \tag{4.33}$$

$$\phi_{2,r}^{(e)}(R, \theta, z) = \begin{cases} -\frac{1}{2}R^2 f_0(\theta)^2 \phi_{0,rrr}^{(e)} - \frac{2f_0(\theta)f_0'(\theta)\phi_{0,\theta}^{(e)}}{R} + f_0(\theta)f_0'(\theta)\phi_{0,r\theta}^{(e)} + \frac{f_1'(\theta)\phi_{0,\theta}^{(e)}}{R} \\ + \frac{f_0'(\theta)\phi_{1,\theta}^{(e)}}{R} - Rf_0(\theta)\phi_{1,rr}^{(e)} - Rf_1(\theta)\phi_{0,rr}^{(e)}, & d \le z \le 1 \\ \phi_{2,r}^{(i)} - \frac{1}{2}R^2 f_0(\theta)^2 \phi_{0,rrr}^{(e)} - \frac{2f_0(\theta)f_0'(\theta)\phi_{0,\theta}^{(e)}}{R} + f_0(\theta)f_0'(\theta)\phi_{0,r\theta}^{(e)} + \frac{f_1'(\theta)\phi_{0,\theta}^{(e)}}{R} \\ + Rf_0(\theta)\phi_{1,rr}^{(e)} + Rf_1(\theta)\phi_{0,rr}^{(e)} + \frac{1}{2}R^2 f_0(\theta)^2 \phi_{0,rrr}^{(i)} + \frac{2f_0(\theta)f_0'(\theta)\phi_{0,\theta}^{(i)}}{R} \\ - f_0(\theta)f_0'(\theta)\phi_{0,r\theta}^{(i)} - \frac{f_1'(\theta)\phi_{0,\theta}^{(i)}}{R} - \frac{f_0'(\theta)\phi_{1,\theta}^{(i)}}{R} + Rf_0(\theta)\phi_{1,rr}^{(i)} + Rf_1(\theta)\phi_{0,rr}^{(i)}, & 0 \le z \le d \end{cases} \tag{4.34}$$

$$\begin{aligned} \phi_2^{(i)}(R, \theta, z) =& \phi_2^{(e)} + \left(\frac{1}{2}R^2 f_0(\theta)^2 \phi_{0,rr}^{(e)} + Rf_0(\theta)\phi_{1,r}^{(e)} + Rf_1(\theta)\phi_{0,r}^{(e)}\right) \\ & - \left(\frac{1}{2}R^2 f_0(\theta)^2 \phi_{0,rr}^{(i)} + Rf_0(\theta)\phi_{1,r}^{(i)} + Rf_1(\theta)\phi_{0,r}^{(i)}\right), \quad 0 \le z \le d \end{aligned} \tag{4.35}$$

$$
\phi_{3,r}^{(e)}(R,\theta,z) = \begin{cases}
-\frac{1}{6}R^3 f_0(\theta)^3\phi_{0,rrrr}^{(e)} - \frac{1}{2}R^2 f_0(\theta)^2\phi_{1,rrr}^{(e)} - R^2 f_1(\theta)f_0(\theta)\phi_{0,rrr}^{(e)} \\
-2f_0(\theta)^2 f_0'(\theta)\phi_{0,r\theta}^{(e)} + \frac{1}{2}Rf_0(\theta)^2 f_0'(\theta)\phi_{0,rr\theta}^{(e)} + \frac{3f_0(\theta)^2 f_0'(\theta)\phi_{0,\theta}^{(e)}}{R} \\
-\frac{2f_0(\theta)f_1'(\theta)\phi_{0,\theta}^{(e)}}{R} - \frac{2f_0(\theta)f_0'(\theta)\phi_{1,\theta}^{(e)}}{R} + f_0(\theta)f_1'(\theta)\phi_{0,r\theta}^{(e)} \\
+f_0(\theta)f_0'(\theta)\phi_{1,r\theta}^{(e)} - \frac{2f_1(\theta)f_0'(\theta)\phi_{0,\theta}^{(e)}}{R} + f_1(\theta)f_0'(\theta)\phi_{0,r\theta}^{(e)} \\
+\frac{f_2'(\theta)\phi_{0,\theta}^{(e)}}{R} + \frac{f_1'(\theta)\phi_{1,r\theta}^{(e)}}{R} + \frac{f_0'(\theta)\phi_{2,\theta}^{(e)}}{R} - Rf_0(\theta)\phi_{2,rr}^{(e)} \\
-Rf_2(\theta)\phi_{0,rr}^{(e)} - Rf_1(\theta)\phi_{1,rr}^{(e)}, & d \le z \le 1 \\
\\
\phi_{3,r}^{(i)} - \frac{1}{6}R^3 f_0(\theta)^3\phi_{0,rrrr}^{(e)} - \frac{1}{2}R^2 f_0(\theta)^2\phi_{1,rrr}^{(e)} \\
-R^2 f_1(\theta)f_0(\theta)\phi_{0,rrr}^{(e)} - 2f_0(\theta)^2 f_0'(\theta)\phi_{0,r\theta}^{(e)} \\
+\frac{1}{2}Rf_0(\theta)^2 f_0'(\theta)\phi_{0,rr\theta}^{(e)} \\
+\frac{3f_0(\theta)^2 f_0'(\theta)\phi_{0,\theta}^{(e)}}{R} - \frac{2f_0(\theta)f_1'(\theta)\phi_{0,\theta}^{(e)}}{R} - \frac{2f_0(\theta)f_0'(\theta)\phi_{1,\theta}^{(e)}}{R} \\
+f_0(\theta)f_1'(\theta)\phi_{0,r\theta}^{(e)} + f_0(\theta)f_0'(\theta)\phi_{1,r\theta}^{(e)} - \frac{2f_1(\theta)f_0'(\theta)\phi_{0,\theta}^{(e)}}{R} \\
+f_1(\theta)f_0'(\theta)\phi_{0,r\theta}^{(e)} + \frac{f_2'(\theta)\phi_{0,\theta}^{(e)}}{R} + \frac{f_1'(\theta)\phi_{1,r\theta}^{(e)}}{R} \\
+\frac{f_0'(\theta)\phi_{2,\theta}^{(e)}}{R} - Rf_0(\theta)\phi_{2,rr}^{(e)} - Rf_2(\theta)\phi_{0,rr}^{(e)} - Rf_1(\theta)\phi_{1,rr}^{(e)} \\
+\frac{1}{6}R^3\phi_{0,rrrr}^{(i)}f_0(\theta)^3 + 2f_0'(\theta)\phi_{0,r\theta}^{(i)}f_0(\theta)^2 \\
-\frac{1}{2}Rf_0'(\theta)\phi_{0,rr\theta}^{(i)}f_0(\theta)^2 \\
+\frac{1}{2}R^2\phi_{1,rrr}^{(i)}f_0(\theta)^2 - \frac{3f_0'(\theta)\phi_{0,\theta}^{(i)}f_0(\theta)^2}{R} + \frac{2f_1'(\theta)\phi_{0,\theta}^{(i)}f_0(\theta)}{R} \\
+\frac{2f_0'(\theta)\phi_{1,\theta}^{(i)}f_0(\theta)}{R} \\
-f_1'(\theta)\phi_{0,r\theta}^{(i)}f_0(\theta) - f_0'(\theta)\phi_{1,r\theta}^{(i)}f_0(\theta) + R\phi_{2,rr}^{(i)}f_0(\theta) \\
+R^2 f_1(\theta)\phi_{0,rrr}^{(i)}f_0(\theta) + \frac{2f_1(\theta)f_0'(\theta)\phi_{0,\theta}^{(i)}}{R} - f_1(\theta)f_0'(\theta)\phi_{0,r\theta}^{(i)} \\
+Rf_2(\theta)\phi_{0,rr}^{(i)} + Rf_1(\theta)\phi_{1,rr}^{(i)} - \frac{f_2'(\theta)\phi_{0,\theta}^{(i)}}{R} - \frac{f_1'(\theta)\phi_{1,\theta}^{(i)}}{R} - \frac{f_0'(\theta)\phi_{2,\theta}^{(i)}}{R}, & 0 \le z \le d
\end{cases} \tag{4.36}
$$

$$
\begin{aligned}
\phi_3^{(i)}(R,\theta,z) =& \phi_3^{(e)} + \frac{1}{6}R^3 f_0(\theta)^3\phi_{0,rrr}^{(e)} + \frac{1}{2}R^2 f_0(\theta)^2\phi_{1,rr}^{(e)} + R^2 f_1(\theta)f_0(\theta)\phi_{0,rr}^{(e)} + Rf_0(\theta)\phi_{2,r}^{(e)} \\
&+ Rf_2(\theta)\phi_{0,r}^{(e)} + Rf_1(\theta)\phi_{1,r}^{(e)} - \frac{1}{6}R^3 f_0(\theta)^3\phi_{0,rrr}^{(i)} - \frac{1}{2}R^2 f_0(\theta)^2\phi_{1,rr}^{(i)} \\
&- R^2 f_1(\theta)f_0(\theta)\phi_{0,rr}^{(i)} + Rf_0(\theta)\phi_{2,r}^{(i)} - Rf_2(\theta)\phi_{0,r}^{(i)} - Rf_1(\theta)\phi_{1,r}^{(i)}, \quad 0 \le z \le d
\end{aligned} \tag{4.37}
$$

4.3. Added Mass and Damping

The velocity potential $\Phi(r, \theta, z, t)$ for a vertical cylinder with circular cross-section is defined as follows:

$$\Phi(r, \theta, z, t) = \bar{h} Re[-i\sigma\bar{\xi}_3 e^{-i\sigma t}\phi(r, \theta, z)] \tag{4.38}$$

The force can be determined by integrating the fluid pressure, $p = -\rho\frac{\partial\Phi}{\partial t}$, over the wetted surface of the cylinder S. The real and imaginary parts of F_z are defined added mass and damping coefficients (Newman (2018)). The added mass coefficient represents the force component proportional to the acceleration and the damping coefficient gives a force proportional to the body velocity.

$$F_z = \iint_S p\mathbf{n}dS = -\rho \iint_S \frac{\partial\Phi}{\partial t}.1dS$$

Note that, $n_z = 1$ and $\bar{r}/\bar{h} = r$.

$$dS = \bar{r}d\bar{r}d\theta$$
$$dS = \bar{h}^2 r dr d\theta$$

$$F_z = +\rho \int_0^{2\pi} \int_0^{R[1+\varepsilon f(\theta)]} \bar{h}^3\sigma^2\bar{\xi}_3 e^{-i\sigma t}\phi(r, \theta, z) r dr d\theta$$

where $max(e^{-i\sigma t}) = 1$.

$$F_z = \sigma^2\bar{\xi}_3\rho\bar{h}^3 \int_0^{2\pi} \int_0^{R[1+\varepsilon f(\theta)]} \phi(r, \theta, z).1 r dr d\theta$$

Note that, $\frac{\partial \phi^{(i)}}{\partial z} = 1$ at $z = d$, $r \leq R[1 + \varepsilon f(\theta)]$.

$$\begin{aligned} F_z &= \sigma^2 \bar{\xi}_3 \rho \bar{h}^3 \int_0^{2\pi} \int_0^{R[1+\varepsilon f(\theta)]} \phi^{(i)}(r,\theta,d) \frac{\partial \phi^{(i)}(r,\theta,d)}{\partial z} r dr d\theta \\ &= \sigma^2 \bar{\xi}_3 \rho \bar{h}^3 \int_0^{2\pi} \int_0^{R[1+\varepsilon f(\theta)]} \phi^{(i)}(r,\theta,d) r dr d\theta \end{aligned} \tag{4.39}$$

The added mass and damping coefficients are related with mass of cylinder. The non-dimensionalized added mass and damping coefficients are

$$\begin{aligned} \mu_{33} + i\lambda_{33} &= \frac{F_z}{\sigma^2 \bar{\xi}_3 \rho \pi \bar{R}^2 (\bar{h} - \bar{d})} \\ &= \frac{1}{\pi R^2 (h-d)} \int_0^{2\pi} \int_0^{R[1+\varepsilon f(\theta)]} \phi^{(i)}(r,\theta,d) r dr d\theta \end{aligned} \tag{4.40}$$

The asmyptotic expansion of $\phi^{(i)}$ in (4.11) substituted into (4.39) and the integration of $\phi_n^{(i)} r$ (with respect to r) are calculated which is denoted by $\tilde{\phi}_n^{(i)}, n = 0, 1, 2$. The limits of the integral are 0 and $R[1 + \varepsilon f(\theta)]$. The result of this integral should be approximated by its Taylor series up to $O(\varepsilon^3)$ at $r = R$. Because we have a problem about dealing with the result $I_m(\lambda_j R[1 + \varepsilon f(\theta)])$. Then, the Fourier series expansion of $f(\theta)$ is substituted. Again, the identity for product of Fourier series in Appendix C is required. The remaining numerical calculations are completed using Mathematica and Matlab.

$$\begin{aligned} \int_0^{R[1+\varepsilon f(\theta)]} \phi^{(i)}(r,\theta,d) r dr &= \int_0^{R[1+\varepsilon f(\theta)]} [\phi_0^{(i)}(r,\theta,d) + \varepsilon \phi_1^{(i)}(r,\theta,d) + \varepsilon^2 \phi_2^{(i)}(r,\theta,d) + O(\varepsilon^3)] r dr \\ &= \tilde{\phi}_0^{(i)}(R[1+\varepsilon f(\theta)],\theta,d) - \tilde{\phi}_0^{(i)}(0,\theta,d) + \varepsilon \tilde{\phi}_1^{(i)}(R[1+\varepsilon f(\theta)],\theta,d) \\ &\quad - \varepsilon \tilde{\phi}_1^{(i)}(0,\theta,d) + \varepsilon^2 \tilde{\phi}_2^{(i)}(R[1+\varepsilon f(\theta)],\theta,d) - \varepsilon^2 \tilde{\phi}_2^{(i)}(0,\theta,d) + O(\varepsilon^3) \\ &= \sum_{n=0}^{2} \varepsilon^n S_n(\theta) + O(\varepsilon^3), \end{aligned}$$

where

$$S_n(\theta) = \frac{1}{2} S_{n0}^{(c)} + \sum_{m=1}^{\infty} S_{nm}^{(c)} \cos(m\theta) + S_{nm}^{(s)} \sin(m\theta)$$

The equation (4.40) gives

$$\mu_{33} + i\lambda_{33} = \frac{1}{\pi R^2(h-d)}(S_{00}^{(c)} + \varepsilon S_{10}^{(c)} + \varepsilon^2 S_{20}^{(c)}) + O(\varepsilon^3), \tag{4.41}$$

where $S_{00}^{(c)}$ is the force on the circular case. As a result of symbolic calculations, we can conclude that $S_{00}^{(c)}$, $S_{10}^{(c)}$ and $S_{20}^{(c)}$ consist of the coefficients α_j, $C_{1,m,j}$ and $C_{2,m,j}$, respectively. The Fourier series of the shape function is necessary for finding the unknown coefficients of interior and exterior potentials in Section 4.2.1. The results of the third-order approximation in equation (4.41) are compared with the previous studies in Section 4.4.

4.4. Added Mass and Damping Coefficients for Vertical Cylinder with Different Cross Section

In this section, non-dimensional added mass and damping coefficients are presented. The asymptotic formulations and the Fourier series are used to calculate radiation force in z direction from a truncated cylinder with elliptic, quasi-elliptic, cosine and square cross-sections in finite water depth.

4.4.1. Added Mass and Damping for Vertical Cylinder with Elliptic Cross Section

The scattering and radiation of gravity waves by an elliptical cylinder is studied by Chen and Mei (1971) that used separation of variables method in elliptical coordinate system and representing the velocity potential in terms of infinite series of Mathieu and modified Mathieu functions. Williams and Darwiche (1990) studied wave radiation from a elliptical cylinder in two cases: cylinder was submerged or floating on the free surface. In their study, a theoretical solution is given for radiation of small amplitude water waves. The numerical results are presented for the added mass and damping coefficients for truncated elliptical cylinders with different eccentricity and drafts. Again, velocity potantial in elliptical coordinates were written in terms of Mathieu and modified Mathieu func-

tions. Yu et al. (2019) studied a semi-analytical model for wave radiation problem from a truncated cylinder with a elliptical cross-section with eccentricity $e = 1/2$ and the non-dimensional area of the elliptic cross-section was 0.25π. Separation of variables method in cylindrical coordinates were used and the velocity potentials were represented in terms of Bessel and modified Bessel functions. In their paper, the potentials were written in terms of Fourier series.

On the other hand, the asymptotic solution of wave diffraction from a bottom-mounted vertical cylinder with elliptic cross-section was presented by Dişibüyük et al. (2017) using the fifth-order and third-order aproximations in case the shape function depend on the small parameter $\varepsilon = e$ in equation (4.29) where e is the elliptic eccentricity. The shape of ellipse closer to circle as e approaches zero. In the case elliptic eccentricity is getting closer to one which means that ellipse is elongated and the method of shape function depend on the small parameter does not provide accurate solution.

In the case of the vertical cylinder with elliptic cross-section which centered at origin and eccentricity $e = \sqrt{1 - b^2/a^2}$. Let a be the semi-major axis on the x-axis and b be the semi-minor axis on the y-axis. The radius function in polar coordinates (r, θ) are given by

$$r = \frac{a\sqrt{1 - e^2}}{\sqrt{1 - e^2\cos^2(\theta)}} \tag{4.42}$$

Let the radius of ellipse be the equation $r = aF(\theta)$, $0 \leq \theta \leq 2\pi$ and $e = \sqrt{1 - (b^2/a^2)} = 0.661437$ since $b/a = 3/4$. First, the Fourier coefficients of $F(\theta)$ should be determined to convert the radius function into the form $r = R[1 + \varepsilon f(\theta)]$ which is the presented asymptotic solution in Section 4.3. We should determine R, ε and Fourier coefficients of $f(\theta)$. The Fourier series of $F(\theta)$ consists of $\cos(2m\theta)$, $m \geq 0$ since the ellipse has two lines of symmetry, $F(\theta) = F(-\theta)$, $F\left(\frac{\pi}{2} - \theta\right) = F\left(\frac{\pi}{2} + \theta\right)$:

$$F(\theta) = \frac{F_0}{2} + \sum_{m=1}^{\infty} F_{2m}\cos(2m\theta), \tag{4.43}$$

$$F_{2m} = \frac{1}{\pi}\int_0^{2\pi} F(\theta)\cos(2m\theta)d\theta = \frac{4}{\pi}\int_0^{\pi/2} F(\theta)\cos(2m\theta)d\theta, \quad m = 0, 1, 2, \ldots$$

The equation $aF(\theta) = R[1 + \varepsilon f(\theta)]$ gives

$$R = aF_0/2 \approx 0.574378$$

The maximum value of $r = aF(\theta)$ is a, so that $\varepsilon = 2/F_0 - 1 \approx 0.160676$ and $|f(\theta)| \leq 1$, where

$$f(\theta) = \sum_{m=1}^{\infty} f_{2m}\cos(2m\theta), \quad f_{2m} = \frac{2F_{2m}}{2 - F_0} \tag{4.44}$$

$f_2 = 0.891393$, $f_4 = 0.0955885$, $f_6 = 0.0113845$, ... The shape of the ellipse with two terms (dashed line) and three terms (dotted line) of (4.44) in equation $r = R[1 + \varepsilon f(\theta)]$ are shown in Figure 4.2. Three terms in the series (4.44) is enough for the ellipse.

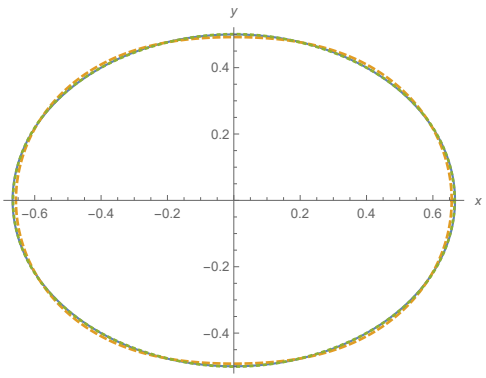

Figure 4.2. Ellipse with eccentricy $e = \sqrt{7}/4$ (solid line) and aproximation of the ellipse by the $r = R[1 + \varepsilon f(\theta)]$ with two terms (dashed line) and three terms (dotted line) in the series (4.44)

First, equation (4.44) is substituted into equations (4.20)-(4.23) to find the unknown coefficients of the interior solution. Secondly, the non-dimensional added mass and damping coefficients in heaving motion are calculated by the third-order approximation in equation (4.41). In this case we should change $(h - d)$ with d in equation (4.41) to compare the non-dimensional results with the paper Williams and Darwiche (1990). Non-dimensional added mass in Figures 4.3(a) and damping in 4.3(b) coefficients for elliptic cross-section with eccentricity $e = \sqrt{7}/4$, $a = 2/3$ and $d = 2/3$. The present asymptotic method of the

third-order in equation (4.41) (solid line) is compared with the solution by Williams and Darwiche (1990) (dots).

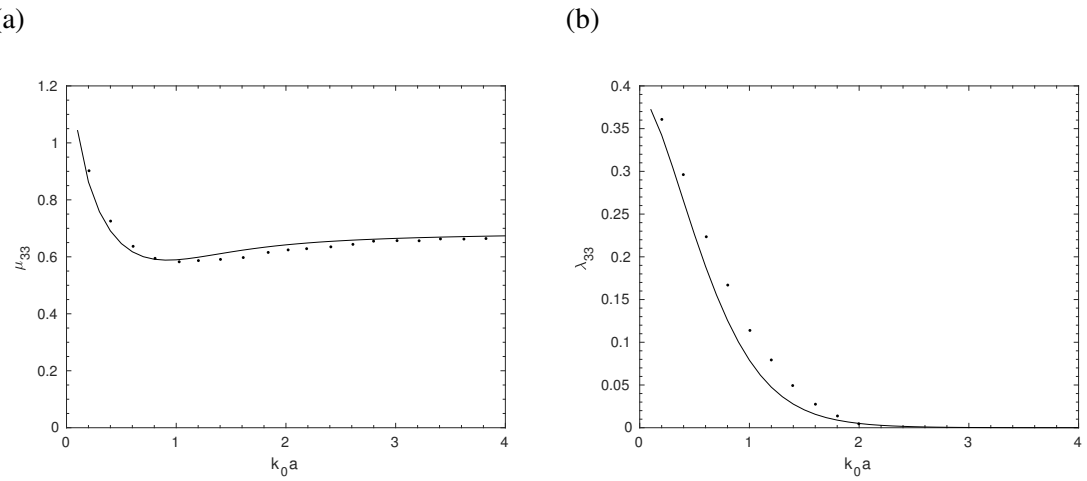

Figure 4.3. Non-dimensional added mass in (a) and damping in (b) coefficients for elliptic cross-section with eccentricity $e = \sqrt{7}/4$ and $d = 2/3$. The present asymptotic method of the third-order (solid line) is compared with the solution by Williams and Darwiche (1990) (dots)

Similarly, we can choose an ellipse with a semi-major axis on the y-axis to compare with the results in the paper Yu et al. (2019). Let a be the semi-major axis on the y-axis and b be the semi-minor axis on the x-axis. The radius function in polar coordinates (r, θ) are given by

$$r = \frac{a\sqrt{1-e^2}}{\sqrt{1-e^2\sin^2(\theta)}} \tag{4.45}$$

Let the radius of ellipse be the equation $r = aF(\theta)$, $0 \leq \theta \leq 2\pi$ and $e = \sqrt{1-(b^2/a^2)} = 0.866025$ since $b/a = 1/2$ and $a = \sqrt{2}/2$. Similarly, the Fourier series of $F(\theta)$ consists of $\cos(2m\theta)$, $m \geq 0$ since the ellipse has two lines of symmetry, $F(\theta) = F(-\theta)$ and $F\left(\frac{\pi}{2} - \theta\right) = F\left(\frac{\pi}{2} + \theta\right)$:

$$F(\theta) = \frac{F_0}{2} + \sum_{m=1}^{\infty} F_{2m}\cos(2m\theta), \tag{4.46}$$

$$F_{2m} = \frac{1}{\pi}\int_0^{2\pi} F(\theta)\cos(2m\theta)d\theta = \frac{4}{\pi}\int_0^{\pi/2} F(\theta)\cos(2m\theta)d\theta, \quad m = 0, 1, 2, \ldots$$

The equation $aF(\theta) = R[1 + \varepsilon f(\theta)]$ gives

$$R = aF_0/2 \approx 0.485387$$

The maximum value of $r = aF(\theta)$ is a, so that $\varepsilon = 2/F_0 - 1 \approx 0.456791$ and $|f(\theta)| \leq 1$, and

$$f(\theta) = \sum_{m=1}^{\infty} f_{2m}\cos(2m\theta) \quad \text{where} \quad f_{2m} = \frac{2F_{2m}}{2 - F_0} \tag{4.47}$$

where $f_2 = -0.74047$, $f_4 = 0.186032$, $f_6 = -0.0518044, \ldots$

The shape of the ellipse with two terms (dotted line) and three terms (dashed line) of (4.47) in equation $r = R[1 + \varepsilon f(\theta)]$ are shown in Figure 4.4. Three terms in the series (4.47) is enough for the ellipse.

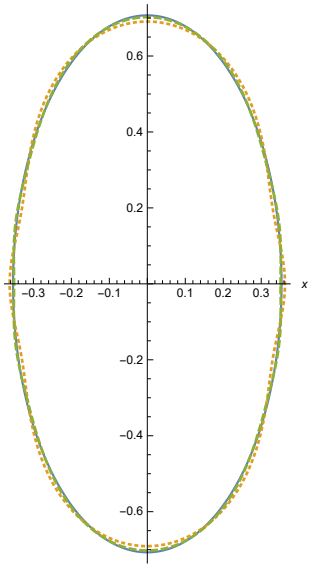

Figure 4.4. Ellipse with eccentricy $e = \sqrt{3}/2$ (solid line) and aproximation of the ellipse by the $r = R[1 + \varepsilon f(\theta)]$ with two terms (dotted line) and three terms (dashed line) in the series (4.47)

As in the first example, equation (4.47) is substituted into equations (4.20)-(4.23) to find the unknown coefficients of the interior solution. Then, the non-dimensional added mass

and damping coefficients in heaving motion are calculated by the third-order approximation in equation (4.41). Non-dimensional added mass in figures 4.5(a) and damping in 4.5(b) coefficients for elliptic cross-section with eccentricity $e = \sqrt{3}/2$ and $d = 0.5$. The present asymptotic method of the second-order (solid line) and the third-order in equation (4.41) (dashed line) is compared with the solution by Yu et al. (2019) (dots).

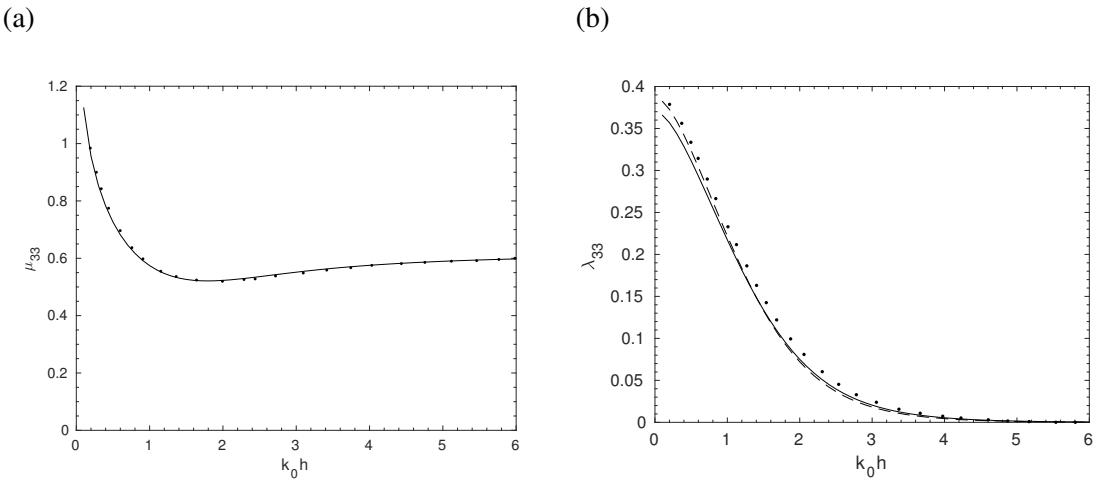

Figure 4.5. Non-dimensional added mass in (a) and damping in (b) coefficients for elliptic cross-section with eccentricity $e = \sqrt{3}/2$ and $d = 0.5$. The present asymptotic method of the second-order (solid line) and the third-order (dashed line) is compared with the solution by Yu et al. (2019) (dots)

The present asymptotic method of the third-order gives good result with the result by Yu et al. (2019). Although the ellipse in the paper Williams and Darwiche (1990) was closer to the circle than the ellipse in the paper Yu et al. (2019), the present asymptotic method in equation (4.41) gives better results for Yu et al. (2019).

4.4.2. Added Mass and Damping for Vertical Cylinder with Quasi-Elliptic Cross Section

A quasi-ellipse contains a rectangle in the middle of two semicirles (Figure 4.6(a)). In this case semicircles on y axis. In Figure 4.6, the length of rectangular part is B and

the radius of the semicircles is $D/2$. The equation $r = F(\theta)$ describes the quasi-ellipse in Figure 4.6(a) in the polar coordinates, where $x = r\cos(\theta)$ and $y = r\sin(\theta)$.

$$F(\theta) = \begin{cases} \frac{D}{2\cos(\theta)}, & 0 \le \theta \le arctan\frac{B}{D} \\ \frac{B\sin(\theta)+\sqrt{D^2-B^2\cos^2(\theta)}}{2}, & arctan\frac{B}{D} \le \theta \le \pi - arctan\frac{B}{D} \\ -\frac{D}{2\cos(\theta)}, & \pi - arctan\frac{B}{D} \le \theta \le \pi + arctan\frac{B}{D} \\ \frac{-B\sin(\theta)+\sqrt{D^2-B^2\cos^2(\theta)}}{2}, & \pi + arctan\frac{B}{D} \le \theta \le 2\pi - arctan\frac{B}{D} \\ \frac{D}{2\cos(\theta)}, & 2\pi - arctan\frac{B}{D} \le \theta \le 2\pi \end{cases}$$

The Fourier coefficients of $F(\theta)$ should be determined to convert the radius function into the form $r = R[1 + \varepsilon f(\theta)]$ which is the presented asymptotic solution in Section 4.3. We should determine R, ε and Fourier coefficients of $f(\theta)$. The Fourier series of $F(\theta)$ consists of $\cos(2m\theta)$, $m \ge 0$ since the quasi-ellipse has two lines of symmetry, $F(\theta) = F(-\theta)$, $F\left(\frac{\pi}{2} - \theta\right) = F\left(\frac{\pi}{2} + \theta\right)$:

$$F(\theta) = \frac{F_0}{2} + \sum_{m=1}^{\infty} F_{2m}\cos(2m\theta), \tag{4.48}$$

$$F_{2m} = \frac{1}{\pi}\int_0^{2\pi} F(\theta)\cos(2m\theta)d\theta = \frac{4}{\pi}\int_0^{\pi/2} F(\theta)\cos(2m\theta)d\theta, \quad m = 0, 1, 2, \ldots$$

Let the non-dimensional area of quasi-ellipse be 0.25π with the axial ratio is 2. We get $B = D$, $D = \sqrt{\pi}/\sqrt{4+\pi}$ and $\arctan(B/D) = 1$. These values were used by Yu et al. (2019). The equation $F(\theta) = R[1 + \varepsilon f(\theta)]$ gives

$$R = F_0/2 \approx 0.484642$$

The maximum value of $r = F(\theta)$ is $(D + B)/2$, so that $\varepsilon = (B + D)/F_0 - 1 \approx 0.368536$ and $|f(\theta)| \le 1$, and

$$f(\theta) = \sum_{m=1}^{\infty} f_{2m}\cos(2m\theta) \quad \text{where} \quad f_{2m} = \frac{2F_{2m}}{\varepsilon F_0} \tag{4.49}$$

where $f_2 = -0.969188$, $f_4 = 0.0776783$, $f_6 = 0.0497145$, ... The shape of the quasi-ellipse with three terms (dashed line) of (4.48) in equation $r = R[1 + \varepsilon f(\theta)]$ is shown in

Figure 4.6(b). Three terms in the series (4.49) is enough for the quasi-ellipse..

(a) (b)

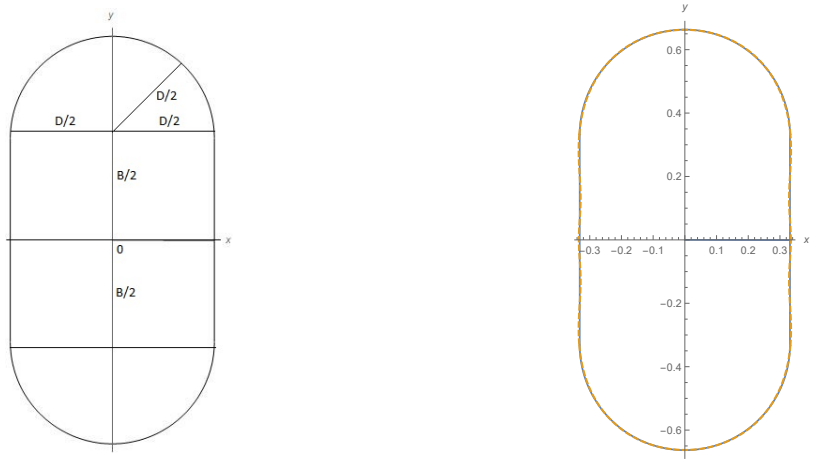

Figure 4.6. (a) Quasi-ellipse, (b) Quasi-ellipse with non-dimensional area is 0.25π and the axial ratio is 2 (solid line) and the approximation by the radius function $r = R[1 + \varepsilon f(\theta)]$ with three terms (dashed line) in the series (4.49)

First, equation (4.49) is substituted into equations (4.20)-(4.23) to find the unknown coefficients of the interior solution. Then, the non-dimensional added mass and damping coefficients in heaving motion are calculated by the third-order approximation in equation (4.41). The present asymptotic method of the third-order in equation (4.41) gives good results with the result by Yu et al. (2019) for added mass for $d = 0.3$, $d = 0.5$, $d = 0.7$ and damping for $d = 0.3$, $d = 0.5$. Damping coefficients approach to zero for $0 < k_0h < 6$ and added mass coefficients approach to a constant (approximately $k_0a > 1$) for all the cases. Also, damping coefficients for different values of d increase whenever d increases (whenever k_0h approaches to zero).

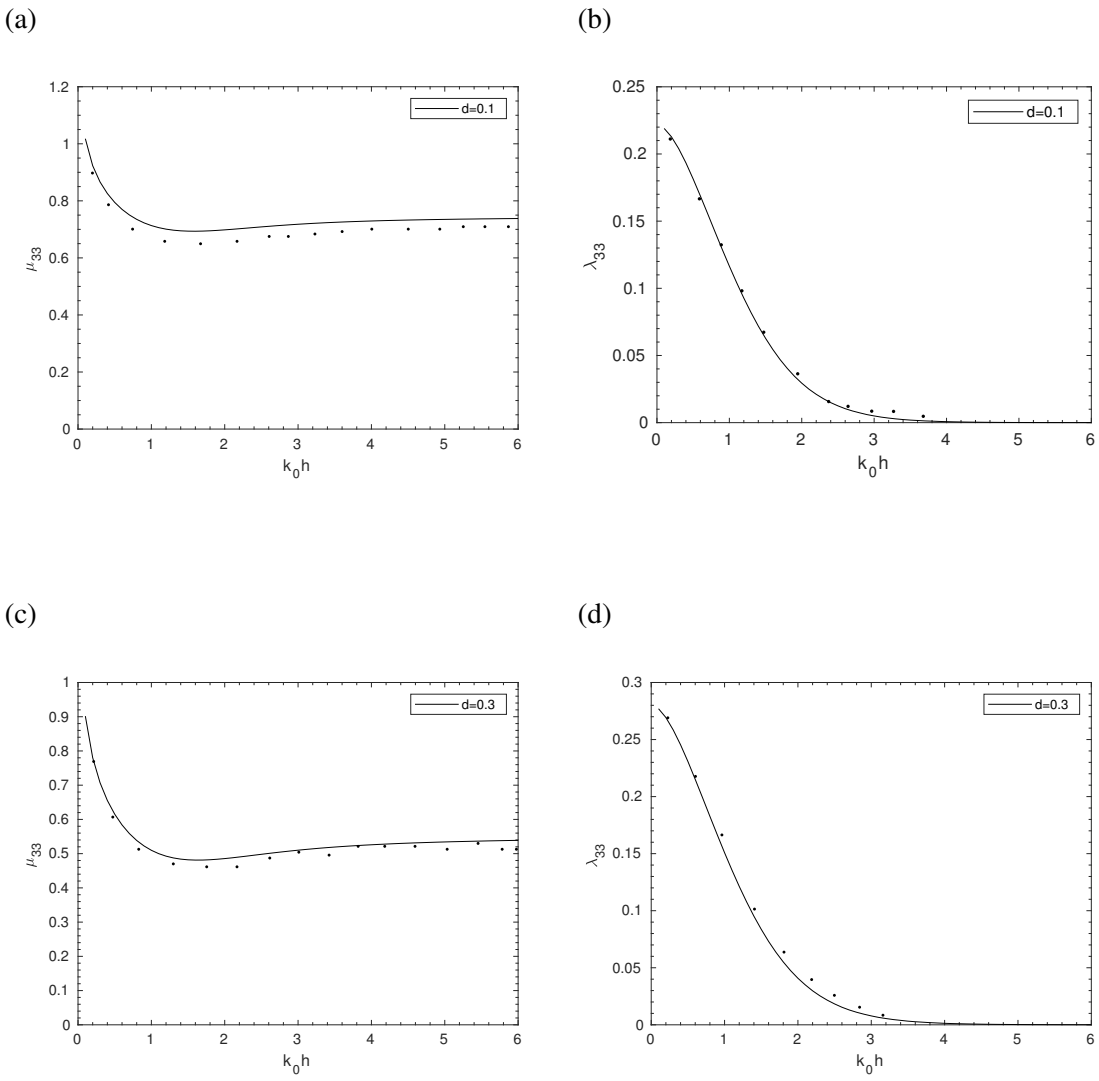

Figure 4.7. Non-dimensional added mass and damping coefficients with $d = 0.1$ and $d = 0.3$ for quasi-elliptic cross-section with the axial ratio is 2 and the non-dimensional area is 0.25π. The present asymptotic method of the third-order (solid line) is compared with the solution by Yu et al. (2019) (dots)

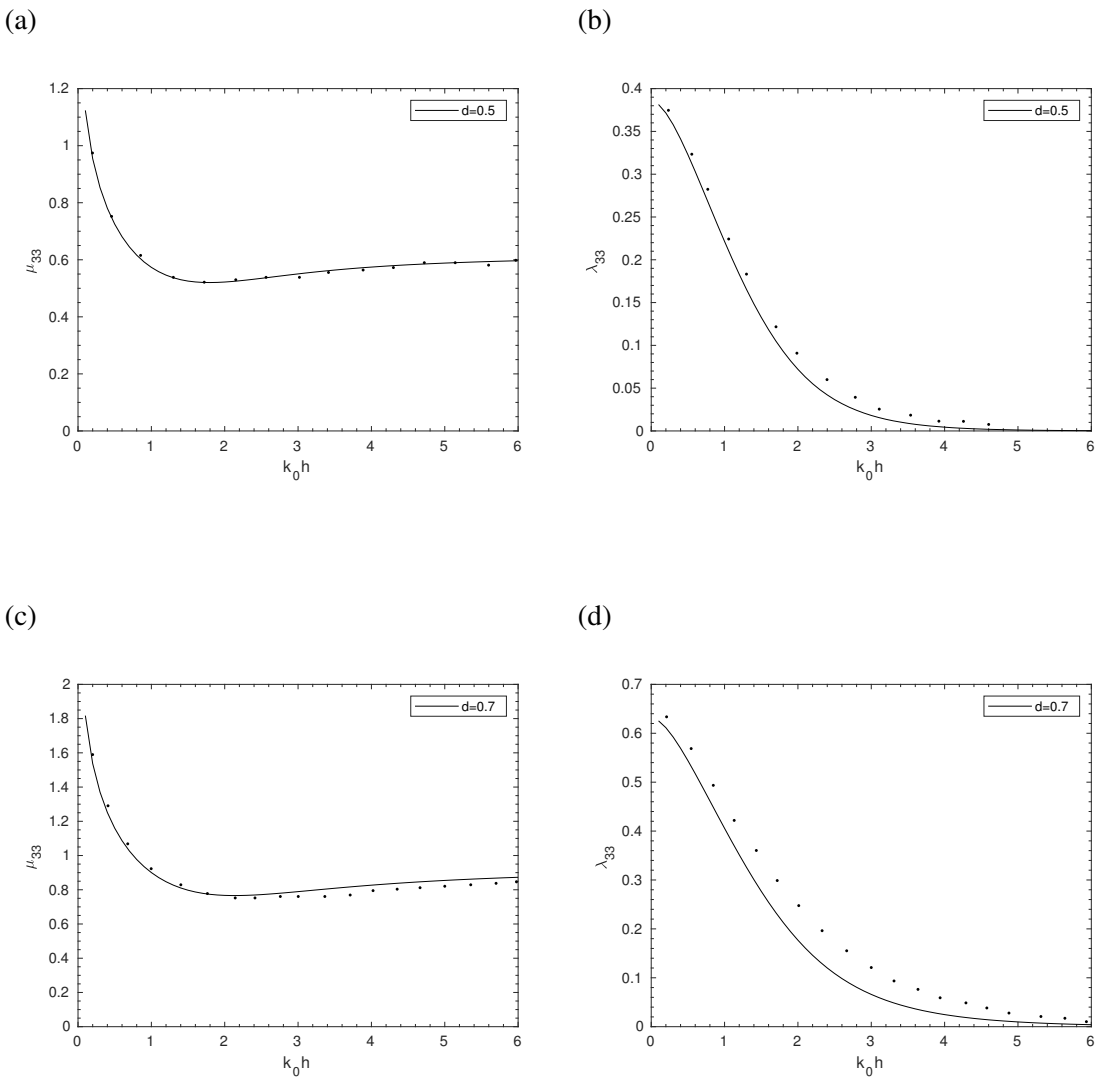

Figure 4.8. Non-dimensional added mass and damping coefficients with $d = 0.5$ and $d = 0.7$ for quasi-elliptic cross-section with the axial ratio is 2 and the non-dimensional area is 0.25π. The present asymptotic method of the third-order (solid line) is compared with the solution by Yu et al. (2019) (dots)

4.4.3. Added Mass and Damping for Vertical Cylinder with Cosine Cross Section

The wave radiation problem for truncated cylinder with cosine cross-section, $r = 0.5[1 + 0.1\cos(3\theta)]$, studied by Yu et al. (2019). In that paper, the numerical results for cosine type radial perturbation were obtained by using the Boundary Element Method and the ANSYS AQWA software showed excellent agreement with the semi-analytical method. The radius of shape function in the form $r = R[1 + \varepsilon f(\theta)]$ is shown in Figure 4.9 which is the presented asymptotic solution in Section 4.3. We have $R = 0.5$, $\varepsilon = 0.1$ and $f(\theta) = \cos(3\theta)$.

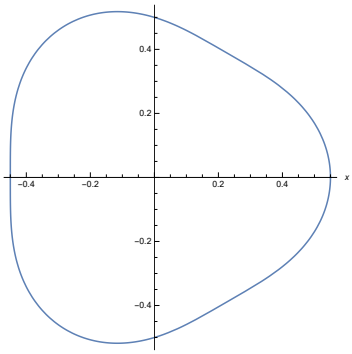

Figure 4.9. The cosine type cross-section with radius $r = 0.5[1 + 0.1\cos(3\theta)]$

In this case, $f(\theta) = \cos(3\theta)$ is substituted into equations (4.20)-(4.23) to find the unknown coefficients of the interior solution. Then, the non-dimensional added mass and damping coefficients in heaving motion are calculated by the third-order approximation in equation (4.41). The present asymptotic method of the third-order in equation (4.41) gives good results with the results by Yu et al. (2019) for added mass and damping with draft $d = 0.5$. Damping coefficients are approaching to zero for $0 < k_0h < 6$ and added mass coefficients are approaching to a constant (approximately $k_0a > 1$).

(a) (b)

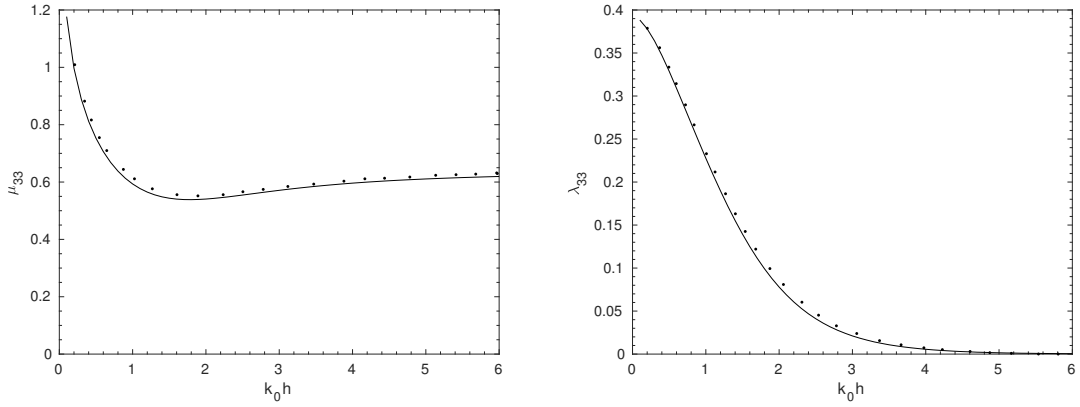

Figure 4.10. Non-dimensional added mass and damping coefficients for cosine type cross-section with $d = 0.5$. The present asymptotic method of the third-order (solid line) is compared with the solution by Yu et al. (2019) (dots)

4.4.4. Added Mass and Damping for Vertical Cylinder with Square Cross Section

Let the radius function of square be the $r = aF(\theta)$, $x = \pm a$, $-a < y < a$ and $y = \pm a$, $-a < x < a$, in the polar coordinates, $x = r\cos(\theta)$, $y = r\sin(\theta)$, since

$$F(\theta) = \begin{cases} \frac{1}{|\cos(\theta)|}, & 0 \le \theta \le \frac{\pi}{4}, \quad \frac{7\pi}{4} \le \theta \le 2\pi \\ \frac{1}{|\sin(\theta)|}, & \frac{\pi}{4} \le \theta \le \frac{3\pi}{4}, \quad \frac{5\pi}{4} \le \theta \le \frac{7\pi}{4} \end{cases}$$

The Fourier coefficients of $F(\theta)$ should be determined to convert the radius function into the form $r = R[1 + \varepsilon f(\theta)]$ which is the presented asymptotic solution in Section 4.3. We should determine R, ε and Fourier coefficients of $f(\theta)$. The Fourier series of $F(\theta)$ consists of $\cos(4m\theta)$, $m \ge 0$ since the quasi-ellipse has four lines of symmetry, $F(\theta) = F(-\theta)$,

$F\left(\frac{\pi}{2}-\theta\right) = F\left(\frac{\pi}{2}+\theta\right)$, $F\left(\frac{\pi}{4}-\theta\right) = F\left(\frac{\pi}{4}+\theta\right)$, $F\left(-\frac{\pi}{4}-\theta\right) = F\left(\frac{\pi}{4}+\theta\right)$:

$$F(\theta) = \frac{F_0}{2} + \sum_{m=1}^{\infty} F_{4m}\cos(4m\theta), \tag{4.50}$$
$$F_{4m} = \frac{8}{\pi}\int_0^{\pi/4} F(\theta)\cos(4m\theta)d\theta \quad m = 0, 1, 2, \ldots$$

Let the non-dimensional area of the square be 0.25π and $a = \sqrt{(\pi/16)} \approx 0.443113$. The equation $F(\theta) = R[1 + \varepsilon f(\theta)]$ gives

$$R = aF_0/2 \approx 0.497262$$

The maximum value of $r = aF(\theta)$ is a, so that $\varepsilon = 2\sqrt{2}/F_0 - 1 \approx 0.260216$ and $|f(\theta)| \leq 1$, and

$$f(\theta) = \sum_{m=1}^{\infty} f_{4m}\cos(4m\theta) \quad \text{where} \quad f_{4m} = \frac{2F_{4m}}{\varepsilon F_0} \tag{4.51}$$

where $f_4 = -0.535742$, $f_8 = 0.168973$, $f_{12} = -0.0801686$, $f_{16} = 0.0463187$, $f_{20} = -0.0300436$, $f_{24} = 0.0210227$, $f_{28} = -0.0155181$, $f_{32} = 0.011918$, $f_{36} = -0.00943701$, $f_{40} = 0.00765587$, ... The shape of the square with four terms (dashed line) and ten terms(dotted line) of (4.51) in equation $r = R[1 + \varepsilon f(\theta)]$ is shown in Figure 4.9. Ten terms in the series (4.51) is enough for the square.

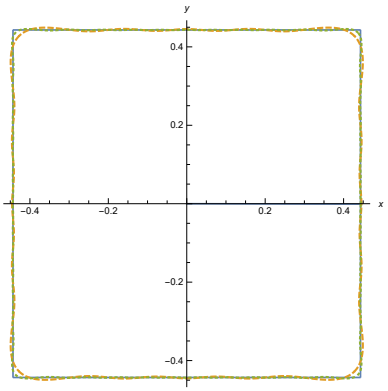

Figure 4.11. The exact shape of the square (solid line) and approximation by the $r = R[1 + \varepsilon f(\theta)]$ with four terms (dashed line) and ten terms (dotted line) in the series (4.51)

First, equation (4.51) is substituted into equations (4.20)-(4.23) to find the unknown coefficients of the interior solution. Then, the non-dimensional added mass and damping coefficients in heaving motion are calculated by the third-order approximation in equation (4.41). The present asymptotic method of the third-order in equation (4.41) is for vertical cylinder with nearly square cross-section for different values of d. Damping coefficients are approaching to zero for $0 < k_0h < 6$ except $d = 0.9$ and added mass coefficients are approaching to a constant (approximately $k_0a > 1$) for all the cases. Also, damping coefficients for different values of d increase whenever d increases (whenever k_0h approaches to zero).

(a) (b)

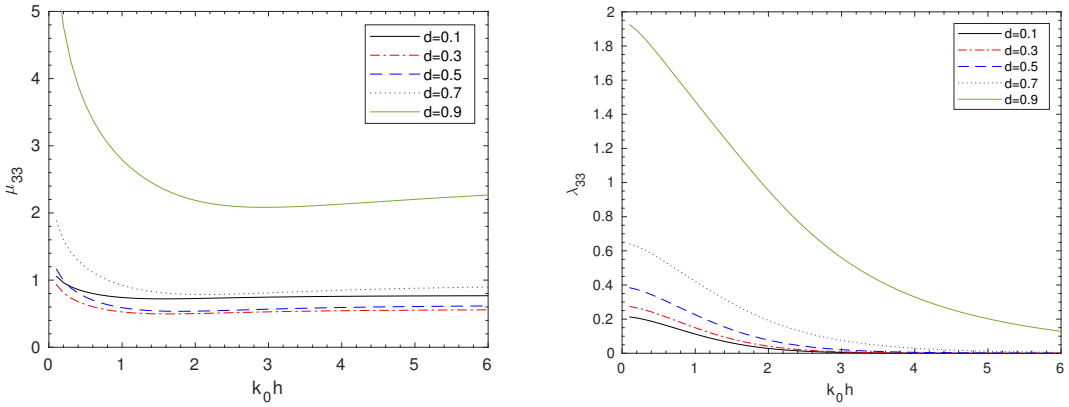

Figure 4.12. Non-dimensional added mass and damping coefficients for vertical cylinder with nearly square cross-section for different values of d. The present asymptotic method of the third-order is used.

4.4.5. Comparison of Added Mass and Damping for Different Cylinders

Wave radiation in heaving motion is studied by the third order asymptotic method. Non-dimensional added mass and damping coefficients are compared for cylinders with circular, cosine type, square, elliptic and quasi-elliptic cross-section (in Figure 4.13) with

same area, i.e., 0.25π. Additionally, axial ratio of elliptic and quasi-elliptic cross-sections is 2.

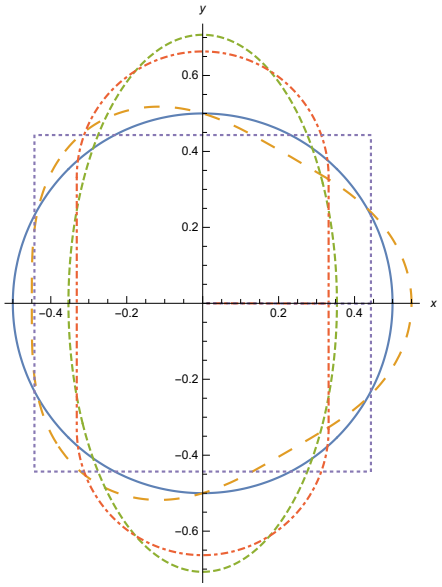

Figure 4.13. Cylinders with circular (solid line), cosine type (large dashed), square (dotted line), elliptic (dashed line) and quasi-elliptic (dotdashed line) cross-section with same area, i.e., 0.25π.

The shape of circular, cosine type and square are close to each other such that added mass and damping coefficients are same in the Figure 4.14. On the other hand, the cylinder with elliptic and quasi-elliptic have almost same added mass and damping coefficients since their cross-section are close. The cylinders with elliptic and quasi-elliptic cross-sections have less added mass and damping than the cylinder with circular, cosine and square cross-sections. Damping coefficients are approaching to zero for $0 < k_0h < 6$ and added mass coefficients are approaching to a constant (approximately $k_0h > 1$) for all the cases.

(a)

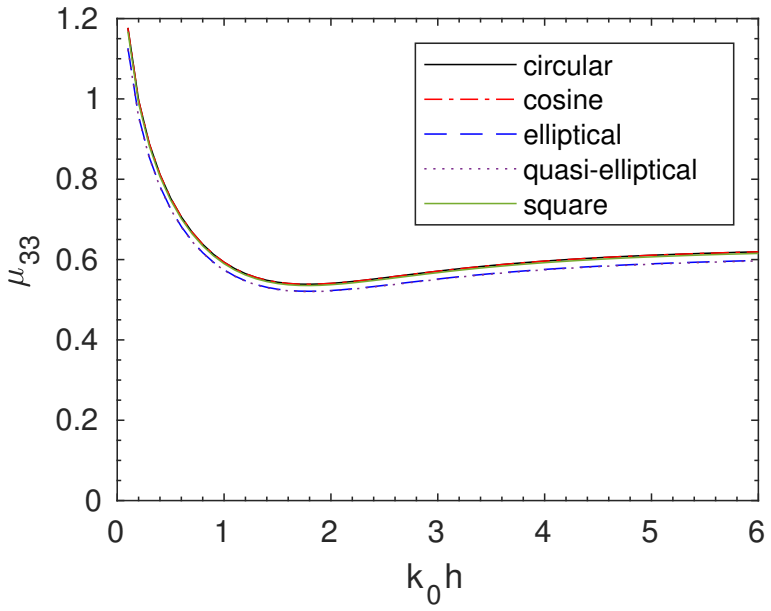

(b)

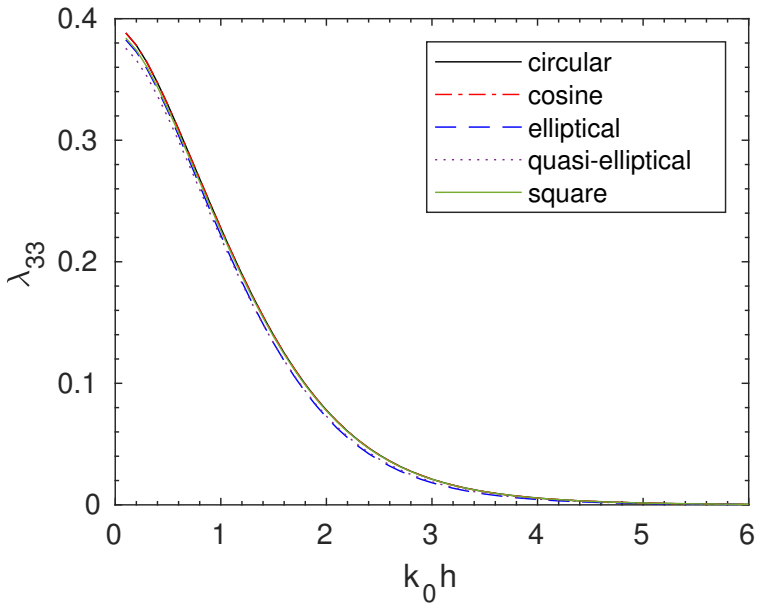

Figure 4.14. Non-dimensional added mass and damping coefficients for different cross-sections with $d = 0.5$

CHAPTER 5

CONCLUSION

Wave radiation problems in heaving motion from a vertical cylinder of circular cross-section and truncated cylinder of an arbitrary cross-section in the water of finite depth are studied. The water domain is divided into two regions: the interior region below the cylinder and the exterior region outside the cylinder. The interior and exterior solutions are matched by the continuity of pressure and normal velocity in both cases.

In Chapter 3, the wave radiation problem in heaving motion by a vertical cylinder of the circular cross-section is solved by using the separation of variables method in cylindrical coordinates. The coefficients of interior and exterior solutions are related to each other by the matching conditions. The matrix system formed by these unknown coefficients has been solved. Then, the non-dimensional z component of force is calculated. Real part and imaginary parts of F_z give added mass and damping coefficients in heaving motion, respectively. Added mass and damping for $0 < k_0a < 4$ presented for different values of radius a and the distance d between sea bottom and cylinder's bottom surface. Added mass coefficients for $a = 5.0$ and $a = 1.0$ are close. Damping coefficients are approaching zero and added mass coefficients are approaching a constant (approximately $k_0a > 1$) for all the cases. Added mass coefficients decrease, whenever d increases. Also, damping coefficients increase whenever d increases (as k_0a approaches zero). However, at the same depth, damping was weakly affected. These numerical results are important for the asymptotic solutions of the present thesis. Because the zeroth-order system of the asymptotic approach is the same as the circular cylinder case.

In Chapter 4, the wave radiation problem in heaving motion by a vertical cylinder of an arbitrary cross-section is solved by an asymptotic approach. The radius of the cross-section of the vertical cylinder is described by the equation $r = R[1 + \varepsilon f(\theta)]$ where R is the mean radius of the cylinder and ε be the small non-dimensional parameter of the problem which is suggested by Dişibüyük et al. (2017). In this thesis, the third-order asymptotic method was obtained. The interior and exterior potentials and shape functions are written in terms of the Fourier Series. The potentials are matched by the

continuity of pressure and normal velocity in both cases. Then the Fourier series of the shape function is written in boundary conditions. The zeroth-order potentials $\phi_0^{(i)}(r,z)$ and $\phi_0^{(e)}(r,z)$ are independent of Fourier coefficients, the first-order potentials $\phi_1^{(i)}(r,\theta,z)$ and $\phi_1^{(e)}(r,\theta,z)$ are linear forms of these coefficients, the second-order potentials $\phi_2^{(i)}(r,\theta,z)$ and $\phi_2^{(e)}(r,\theta,z)$ are quadratic forms of these coefficients. When the force in the z-direction is calculated after the necessary asymptotic and Taylor series expansions, it includes the constant coefficients of interior potentials. Non-dimensional added mass and damping coefficients are compared for cylinders with circular, cosine type, square, elliptic, and quasi-elliptic cross-section with the other numerical results. The shape of circular, cosine type and square are close to each other such that added mass and damping coefficients are the same. On the other hand, the cylinder with elliptic and quasi-elliptic have almost same added mass and damping coefficients since their cross-sections are close. The cylinders with elliptic and quasi-elliptic cross-sections have less added mass and damping than the cylinder with circular, cosine and square cross-sections. Damping coefficients are approaching zero for $0 < k_0h < 6$ and added mass coefficients are approaching a constant (approximately $k_0h > 1$) for all the cases.

The advantages of this method are the higher orders can be solved sequentially using hydrodynamic coefficients of the circular cylinder and Fourier Series. This method can be applied in geometries where the Fourier series of the shape function is known. The cross-section of the cylinder can be written as a Fourier Series and the method gives better results if the value of ε is small. The disadvantages of this method are when epsilon is close to one; the method does not give good results with other numerical calculations. As the number of orders of the asymptotic approach increases, the numbers of terms increase, and solving systems of equations slows down.

REFERENCES

Abramowitz, M. and I. A. Stegun (1970). *Handbook of Mathematical Functions with Formulas, Graphs, and Mathematical Tables (9th edition)*. New York: Dover.

Acheson, D. J. (2005). *Elementary Fluid Dynamics*. Oxford University Press.

Bhatta, D. D. (2007). Computation of added mass and damping coefficients due to a heaving cylinder. *Journal of Applied Mathematics and Computing 23*(1-2), 127–140.

Black, J. L., C. C. Mei, and M. C. G. Bray (1971). Radiation and scattering of water waves by rigid bodies. *Journal of Fluid Mechanics 46*(1), 151–164.

Chen, H. S. and C. C. Mei (1971). Scattering and radiation of gravity waves by an elliptical cylinder. Technical report, MIT.

Dişibüyük, N. B., A. Korobkin, and O. Yilmaz (2017). Linear wave interaction with a vertical cylinder of arbitrary cross section: an asymptotic approach. *Journal of Waterway, Port, Coastal, and Ocean Engineering 143*(5), 04017028.

Drobyshevski, Y. (2004). Hydrodynamic coefficients of a floating, truncated vertical cylinder in shallow water. *Ocean engineering 31*(3-4), 269–304.

Eidem, M. E. (2017). Overview of floating bridge projects in Norway. In *International Conference on Offshore Mechanics and Arctic Engineering*, Volume 57779, pp. V009T12A018. American Society of Mechanical Engineers.

Fichtenholz, G. M. (2001). *A Course in Differential and Integral Calculus, Vol. 3*. Fizmatlit, Moscow.

Garrett, C. (1971). Wave forces on a circular dock. *Journal of Fluid Mechanics 46*(1), 129–139.

Haskind, M. D. (1957). The exciting forces and wetting of ships in waves. *(in Russian),*

Izvestia Akademii Nauk S.S.S.R., Otdelenie Tekhnicheskikh Nauk (7), 65–79.

Islam, H., S. Mohapatra, J. Gadelho, and C. G. Soares (2019). Openfoam analysis of the wave radiation by a box-type floating structure. *Ocean Engineering 193*, 106532.

Jiang, S. C., Y. Gou, and B. Teng (2014). Water wave radiation problem by a submerged cylinder. *Journal of Engineering Mechanics 140*(5), 06014003.

Lee, J. F. (1995). On the heave radiation of a rectangular structure. *Ocean Engineering 22*(1), 19–34.

Linton, C., D. Evans, and F. Smith (1992). The radiation and scattering of surface waves by a vertical circular cylinder in a channel. *Philosophical Transactions of the Royal Society of London. Series A: Physical and Engineering Sciences 338*(1650), 325–357.

Liu, J., A. Guo, Q. Fang, H. Li, H. Hu, and P. Liu (2018). Investigation of linear wave action around a truncated cylinder with non-circular cross section. *Journal of Marine Science and Technology 23*(4), 866–876.

Liu, J., A. Guo, and H. Li (2016). Analytical solution for the linear wave diffraction by a uniform vertical cylinder with an arbitrary smooth cross-section. *Ocean Engineering 126*, 163–175.

Mansour, A. M., A. N. Williams, and K. Wang (2002). The diffraction of linear waves by a uniform vertical cylinder with cosine-type radial perturbations. *Ocean engineering 29*(3), 239–259.

Mei, C. C. (1978). Numerical methods in water-wave diffraction and radiation. *Annual Review of Fluid Mechanics 10*(1), 393–416.

Mei, C. C., M. Stiassnie, and D. K.-P. Yue (2005). *Theory and applications of ocean surface waves: nonlinear aspects*, Volume 23. World scientific.

Newman, J. N. (2018). *Marine hydrodynamics*. MIT press.

Shen, Y., Y. Zheng, and Y. You (2005). On the radiation and diffraction of linear water waves by a rectangular structure over a sill. part i. infinite domain of finite water depth. *Ocean Engineering 32*(8-9), 1073–1097.

Sudhakar, S. and S. Nallayarasu (2011). Influence of heave plate on hydrodynamic response of spar. In *International Conference on Offshore Mechanics and Arctic Engineering*, Volume 44335, pp. 437–447.

Wan, L., A. R. Magee, Ø. Hellan, W. Arnstein, K. K. Ang, and C. M. Wang (2017). Initial design of a double curved floating bridge and global hydrodynamic responses under environmental conditions. In *ASME 2017 36th International Conference on Ocean, Offshore and Arctic Engineering*. American Society of Mechanical Engineers Digital Collection.

Williams, A. and M. Darwiche (1990). Wave radiation by truncated elliptical cylinder. *Journal of waterway, port, coastal, and ocean engineering 116*(1), 101–119.

Yeung, R. W. (1981). Added mass and damping of a vertical cylinder in finite-depth waters. *applied ocean research 3*(3), 119–133.

Yu, H., S. Zheng, Y. Zhang, and G. Iglesias (2019). Wave radiation from a truncated cylinder of arbitrary cross section. *Ocean Engineering 173*, 519–530.

Zhang, S., A. Williams, et al. (1995). Wave radiation by a submerged elliptical disk. In *The Fifth International Offshore and Polar Engineering Conference*. International Society of Offshore and Polar Engineers.

Zheng, S. and Y. Zhang (2016). Wave radiation from a truncated cylinder in front of a vertical wall. *Ocean Engineering 111*, 602–614.

Zheng, S. and Y. Zhang (2018). Theoretical modelling of a new hybrid wave energy converter in regular waves. *Renewable Energy 128*, 125–141.

Zheng, Y., Y. Shen, Y. You, B. Wu, and D. Jie (2006). Wave radiation by a floating

rectangular structure in oblique seas. *Ocean Engineering 33*(1), 59–81.

Zheng, Y., Y. You, and Y. Shen (2004). On the radiation and diffraction of water waves by a rectangular buoy. *Ocean engineering 31*(8-9), 1063–1082.

APPENDIX A

THE FUNCTION Z_ℓ NORMALIZED IN [0,1]

$$Z_\ell(k_\ell z) = \begin{cases} cosh(k_0 z)/N_0^{1/2}, & N_0 = \frac{1}{2}(1 + \frac{sinh(2k_0)}{2k_0}) \\ cos(k_\ell z)/N_\ell^{1/2}, & N_\ell = \frac{1}{2}(1 + \frac{sin(2k_\ell)}{2k_\ell}) \end{cases} \tag{A.1}$$

The function $\langle Z_\ell(k_\ell z), Z_j(k_j z)\rangle$ is normalized orthogonal set in [0,1] as shown below

$$\begin{aligned} \int_0^1 [Z_0(k_0 z)]^2 dz &= \int_0^1 \frac{cosh(2k_0 z) + 1}{2N_0} dz \\ &= \frac{\frac{sinh(2k_0 z)}{2k_0} + z}{2N_0}\Big|_0^1 = \frac{\frac{sinh(2k_0)}{2k_0} + 1}{2N_0} = 1 \end{aligned} \tag{A.2}$$

For $\ell = 1, 2, 3, ...$, we have

$$\begin{aligned} \int_0^1 [Z_\ell(k_\ell z)]^2 dz &= \int_0^1 \frac{cos(2k_\ell z) + 1}{2N_\ell} dz \\ &= \frac{\frac{sin(2k_\ell z)}{2k_\ell} + z}{2N_\ell}\Big|_0^1 = \frac{\frac{sin(2k_\ell)}{2k_\ell} + 1}{2N_\ell} = 1 \end{aligned} \tag{A.3}$$

$$\begin{aligned} \int_0^1 Z_0(k_0 z) Z_\ell(k_\ell z) dz &= \int_0^1 \frac{cosh(k_0 z) cos(k_\ell z)}{N_0^{1/2} N_\ell^{1/2}} dz \\ &= \frac{sinh(k_0 z) cos(k_\ell z)}{k_0 N_0^{1/2} N_\ell^{1/2}}\Big|_0^1 - \int_0^1 \frac{k_\ell sinh(k_0 z) sin(k_\ell z)}{k_0 N_0^{1/2} N_\ell^{1/2}} dz \\ &= \frac{sinh(k_0 z) cos(k_\ell z)}{k_0 N_0^{1/2} N_\ell^{1/2}}\Big|_0^1 + \frac{k_\ell cosh(k_0 z) sin(k_\ell z)}{k_0^2 N_0^{1/2} N_\ell^{1/2}}\Big|_0^1 - \frac{k_\ell^2}{k_0^2} \int_0^1 \frac{cosh(k_0 z) cos(k_\ell z)}{N_0^{1/2} N_\ell^{1/2}} dz \end{aligned}$$

$$\int_0^1 \frac{cosh(k_0 z) cos(k_\ell z)}{N_0^{1/2} N_\ell^{1/2}} dz = \left(\frac{sinh(k_0) cos(k_\ell)}{k_0 N_0^{1/2} N_\ell^{1/2}} + \frac{k_\ell cosh(k_0) sin(k_\ell)}{k_0^2 N_0^{1/2} N_\ell^{1/2}} \right) / \left(1 + \frac{k_\ell^2}{k_0^2} \right) \tag{A.4}$$

We can rearrange the right-hand side of the equation (A.4) to use the dispersion relations $k_0 tanh(k_0) = v$ and $k_\ell tan(k_\ell) = -v$,

$$\begin{aligned}\frac{sinh(k_0)cos(k_\ell)}{k_0 N_0^{1/2} N_\ell^{1/2}} + \frac{k_\ell cosh(k_0)sin(k_\ell)}{k_0^2 N_0^{1/2} N_\ell^{1/2}} &= \frac{sinh(k_0)cos(k_\ell)}{k_0 N_0^{1/2} N_\ell^{1/2}} \left(1 + \frac{k_\ell tan(k_\ell)}{k_0 tanh(k_0)}\right) \\ &= \frac{sinh(k_0)cos(k_\ell)}{k_0 N_0^{1/2} N_\ell^{1/2}} \left(1 + \frac{-v}{v}\right) = 0\end{aligned}$$

So that,

$$\int_0^1 Z_0(k_0 z) Z_\ell(k_\ell z) dz = 0 \tag{A.5}$$

For $\ell = 1, 2, 3, \ldots$, $j = 1, 2, 3, \ldots$, $\ell \neq j$ and we have

$$\begin{aligned}\int_0^1 Z_\ell(k_\ell z) Z_j(k_j z) dz &= \int_0^1 \frac{cos(k_\ell z) cos(k_j z)}{N_\ell^{1/2} N_j^{1/2}} dz \\ &= \int_0^1 \frac{cos(k_\ell z + k_j z) + cos(k_\ell z - k_j z)}{2 N_\ell^{1/2} N_j^{1/2}} dz \\ &= \frac{sin(k_\ell z + k_j z)}{2 N_\ell^{1/2} N_j^{1/2} (k_\ell z + k_j z)}\Big|_0^1 + \frac{sin(k_\ell z - k_j z)}{2 N_\ell^{1/2} N_j^{1/2} (k_\ell z - k_j z)}\Big|_0^1 \\ &= \frac{sin(k_\ell + k_j)}{2 N_\ell^{1/2} N_j^{1/2} (k_\ell + k_j)} + \frac{sin(k_\ell - k_j)}{2 N_\ell^{1/2} N_j^{1/2} (k_\ell - k_j)} \\ &= \frac{(k_\ell - k_j) sin(k_\ell + k_j) + (k_\ell + k_j) sin(k_\ell - k_j)}{2 N_\ell^{1/2} N_j^{1/2} (k_\ell^2 - k_j^2)}\end{aligned}$$

We can use sum and difference formulas for sine,

$$\begin{aligned}(k_\ell - k_j) sin(k_\ell + k_j) + (k_\ell + k_j) sin(k_\ell - k_j) &= 2(k_\ell sin(k_\ell) cos(k_j) - k_j cos(k_\ell) sin(k_j)) \\ &= 2k_\ell sin(k_\ell) cos(k_j) \left(1 - \frac{k_j tan(k_j)}{k_\ell tan(k_\ell)}\right) \\ &= 2k_\ell sin(k_\ell) cos(k_j) \left(1 - \frac{(-v)}{(-v)}\right) = 0\end{aligned}$$

$$\int_0^1 Z_\ell(k_\ell z) Z_j(k_j z) dz = 0 \tag{A.6}$$

So, the inner product $\left\langle Z_\ell, Z_j \right\rangle = \delta_{\ell j}$, where $\delta_{\ell j}$ is the Kronecker delta.

$$\delta_{\ell j} = \begin{cases} 0 & , \ \ell \neq j \\ 1 & , \ \ell = j \end{cases} \tag{A.7}$$

APPENDIX B

DEFINITION AND PROPERTIES OF MODIFIED BESSEL FUNCTION *I*

$$z^2\frac{d^2w}{dz^2} + z\frac{dw}{dz} - (z^2 + v^2)w = 0$$

Solutions of the differential equation are modifed Bessel functions $I_{\pm v}(z)$ and $K_v(z)$. $I_v(z)$ is called the modified Bessel function of order v of the first kind.

$$\frac{\partial I_v(z)}{\partial z} = \frac{v}{z}I_v(z) + I_{v+1}(z)$$

So, we get

$$\frac{\partial I_0(z)}{\partial z} = I_1(z) \tag{B.1}$$

$$\int_0^z tI_0(t)dt = zI_1(z) \tag{B.2}$$

from (9.6.27) and (11.3.25) in Abramowitz and Stegun (1970).

APPENDIX C

THE PRODUCT OF TWO FOURIER SERIES

The product of two Fourier series gives a Fourier series. Dişibüyük et al. (2017) used for the product of Fourier series in the system of equations of diffraction problem.

$$f(\theta) \sim \frac{a_0}{2} + \sum_{m=1}^{\infty} a_m cos(m\theta) + b_m sin(m\theta)$$

$$g(\theta) \sim \frac{c_0}{2} + \sum_{m=1}^{\infty} c_m cos(m\theta) + d_m sin(m\theta) \tag{C.1}$$

$$f(\theta)g(\theta) \sim \frac{A_0}{2} + \sum_{m=1}^{\infty} A_m cos(m\theta) + B_m sin(m\theta)$$

where Fichtenholz (2001)

$$A_n = \frac{a_0 c_n}{2} + \frac{1}{2}\sum_{m=1}^{\infty}[a_m(c_{m+n} + c_{m-n}) + b_m(d_{m+n} + d_{m-n})] \tag{C.2}$$

$$B_n = \frac{a_0 d_n}{2} + \frac{1}{2}\sum_{m=1}^{\infty}[a_m(d_{m+n} + d_{m-n}) - b_m(c_{m+n} - c_{m-n})] \tag{C.3}$$

$d_{m-n} = -d_{n-m}$ and $a_{m-n} = a_{n-m}$ if $m - n < 0$.

APPENDIX D

BEHAVIOUR OF α_J AND A_ℓ FOR VARYING NUMBER OF EQUATIONS

Table D.1. Behaviour of α_j and A_ℓ for variying number of equations

$N = 5$, $d = 0.5$, $a = 0.5$, $k_0 = 1.0$,
$(\mu_{33}, \lambda_{33}) = (0.61354, 0.22437)$

	α_j		A_ℓ	
	Re	*Im*	*Re*	*Im*
0	0.3994	0.2176	0.1727	0.0051
1	-0.0022	0.0001	-1.4472	0.0636
2	0.1240	-0.0054	-8.8840	0.3306
3	-0.0372	0.0015	-20.4621	0.9664
4	0.0156	-0.0005	-37.1218	2.4864

$N = 10$, $d = 0.5$, $a = 0.5$, $k_0 = 1.0$,
$(\mu_{33}, \lambda_{33}) = (0.61052, 0.22444)$

	α_j		A_ℓ	
	Re	*Im*	*Re*	*Im*
0	0.3995	0.2175	0.1706	0.0052
1	-0.0004	0.00001	-1.4651	0.0647
2	0.1252	-0.0054	-8.9842	0.3354
3	-0.0347	0.0014	-21.6485	0.9895
4	0.0157	-0.0006	-48.4433	2.9390

$N = 20$, $d = 0.5$, $a = 0.5$, $k_0 = 1.0$,
$(\mu_{33}, \lambda_{33}) = (0.60979, 0.22447)$

	α_j		A_ℓ	
	Re	*Im*	*Re*	*Im*
0	0.3991	0.2175	0.1704	0.0052
1	-0.0004	0.000008	-1.4660	0.0649
2	0.1252	-0.0055	-8.9912	0.3358
3	-0.0341	0.0014	-21.8397	0.9948
4	0.0156	-0.0006	-50.2130	3.0113